Journal of Pharmaceutical Analysis 9 (2019) 373–391

Contents lists available at ScienceDirect

Journal of Pharmaceutical Analysis

journal homepage: www.elsevier.com/locate/jpa

Review Paper

Analytical methodologies for determination of methotrexate and its metabolites in pharmaceutical, biological and environmental samples

Forough Karami [a, b, c, 1], Sara Ranjbar [a, 1, *], Younes Ghasemi [a, d, **], Manica Negahdaripour [a]

[a] Pharmaceutical Sciences Research Center, Shiraz University of Medical Sciences, Shiraz, Iran
[b] Central Research Laboratory, School of Medicine, Shiraz University of Medical Sciences, Shiraz, Iran
[c] Chemistry Department, Yasouj University, Yasouj, Iran
[d] Department of Pharmaceutical Biotechnology, School of Pharmacy, Shiraz University of Medical Sciences, Shiraz, Iran

ARTICLE INFO

Article history:
Received 23 February 2019
Received in revised form
5 May 2019
Accepted 19 June 2019
Available online 20 June 2019

Keywords:
Methotrexate
Antifolate
Anticancer
Quantification
High performance liquid chromatography

ABSTRACT

Methotrexate (MTX) is a folate antagonist drug used for several diseases, such as cancers, various malignancies, rheumatoid arthritis (RA) and inflammatory bowel disease. Due to its structural features, including the presence of two carboxylic acid groups and its low native fluorescence, there are some challenges to develop analytical methods for its determination. MTX is metabolized to 7-hydroxymethotrexate (7-OH-MTX), 2,4-diamino-N10-methylpteroic acid (DAMPA), and the active MTX polyglutamates (MTXPGs) in the liver, intestine, and red blood cells (RBCs), respectively. Additionally, the drug has a narrow therapeutic range; hence, its therapeutic drug monitoring (TDM) is necessary to regulate the pharmacokinetics of the drug and to decrease the risk of toxicity. Due to environmental toxicity of MTX; its sensitive, fast and low cost determination in workplace environments is of great interest. A large number of methodologies including high performance liquid chromatography equipped with UV–visible, fluorescence, or electrochemical detection, liquid chromatography-mass spectroscopy, capillary electrophoresis, UV–visible spectrophotometry, and electrochemical methods have been developed for the quantitation of MTX and its metabolites in pharmaceutical, biological, and environmental samples. This paper will attempt to review several published methodologies and the instrumental conditions, which have been applied to measure MTX and its metabolites within the last decade.

1. Introduction

Methotrexate (MTX), 4-amino-N10-methylpteroylglutamic acid, is an antifolate drug, developed as the first targeted anticancer agent in 1940 [1]. It is administered at a high dose to treat several types of cancers, such as acute human leukemia, breast cancer, osteogenic sarcoma, head and neck carcinomas, prostate and bladder cancers [2–5]. It is also administered at a low dose as a remedy for a variety of autoimmune and inflammatory diseases, such as rheumatoid arthritis (RA), psoriasis, sarcoidosis, and systemic lupus erythematosus [6].

MTX is produced by several companies; hence, to provide high quality, safe and effective products, quality control is essential in the pharmaceutical industry [7]. As the range between minimal effective concentration (MEC) and minimal toxic concentration (MTC) of MTX is considerably small, the drug has a narrow therapeutic range [8]. High therapeutic concentrations might lead to hepatic and pulmonary anomaly and myelosuppresion [9–12]. In addition, renal toxicity may occur due to precipitation of MTX and its less soluble metabolites, 7-hydroxymethotrexate (7-OH-MTX) and 2,4-diamino-N10-methylpteroic acid (DAMPA), in urine [13,14]. Therefore, therapeutic drug monitoring (TDM) of MTX is needed to monitor its pharmacokinetics and to decrease the risk of toxicity. Moreover, due to its environmental toxicity, in the last decade research has focused on determining MTX at trace levels in the workplace environments, such as industries and pharmacies, and in the sewage waters from hospitals [15,16]. To this end, numerous analytical methodologies have reported the analysis of MTX in

Peer review under responsibility of Xi'an Jiaotong University.
* Corresponding author.
** Corresponding author at: Pharmaceutical Sciences Research Center, Shiraz University of Medical Sciences, Shiraz, Iran.
E-mail addresses: ranjbar18@yahoo.com (S. Ranjbar), Ghasemiy@sums.ac.ir (Y. Ghasemi).
[1] These two authors contributed equally to this work and both considered as the first author.

https://doi.org/10.1016/j.jpha.2019.06.001

various fields, such as formulation quality control, TDM and environmental contaminants.

The aim of this study was to provide an overview of the analytical techniques to determine MTX and its metabolites in pharmaceutical, biological and environmental samples, reported in the literature within the last decade.

2. Chemical properties of methotrexate

MTX structure is very similar to that of folic acid (FA). MTX consists of a petridine-diamine core and a p-aminobenzoyl portion, linked to a glutamic acid part containing two highly ionizable carboxylic acid groups. Its solubility is pH-dependent, as neutral or basic solutions are required for its solubility. The presence of an asymmetric carbon in the structure results in S and R stereoisomers. S-MTX is considered as the active form, while R isomer is introduced as the impurity [17]. The structures of FA, and MTX and its three main metabolites are depicted in Fig. 1.

3. Pharmacology of MTX

MTX inhibits dihydrofolate reductase enzyme reversibly, and leads to the depletion of reduced folates, which plays a crucial role in methionine, thymidylate, and purine biosynthesis. Subsequently, the reduction of nucleotides suppresses the DNA synthesis in cancerous cells. In addition, MTX inhibits folate-dependent enzymes (thymidylate synthase) by dihydrofolate metabolites and the polyglutamate forms of MTX [18,19]. Rephrase MTX is administered *via* various routes including oral, intravenous, subcutaneous, intramuscular, and intrathecal ones with wide variations of dosing (from 7.5 mg to 12 g/m^2) depending on tumor type, body size, patient age, and the protocol followed [20]. The oral absorption is nearly complete in doses of up to 30 mg/m^2. In high-dose regimens, the drug is administered intravenously due to the reduced absorption in doses greater than 30 mg/m^2 [21]. In the liver, MTX is converted to the major active metabolite, 7-OH-MTX [22]. In the intestine, MTX is metabolized to DAMPA and glutamic acid. MTX can also be taken-up by red blood cells (RBCs), where it undergoes polyglutamation. MTX conversion into MTXPGs takes place in the cells by folylpolyglutamate synthase [23,24]. Since the amount of intracellular MTXPGs is related to efficacy and toxicity of MTX, MTXPGs monitoring is important when assessing the pharmacokinetic–pharmacodynamic profile of MTX in RA treatment, psoriasis, ankylosing spondylitis, and cancer [25–29]. MTX is mainly eliminated by the kidneys and the clearance displays great variations according to age, race, gender, regimen, and renal function [30]. Some disorders, such as malignant effusions and hypoalbuminemia, affect MTX elimination [31,32]. The most important side effects of MTX treatment are hematologic, hepatic, gastrointestinal, and mucosal events. In addition, high doses of MTX might induce kidney injury due to crystallization of the parent drug and the metabolites in the nephrons, and the retardation of renal elimination leads to systemic toxicity [33].

4. Sample treatment procedures

As sample preparation is often the rate-limiting and labor-intensive step of the whole analytical procedure, choosing an optimal technique for sample preparation is the most significant step in setting up an analytical method for the measurement of MTX in different samples. It seems that the direct injection of biological samples to liquid chromatography (LC) columns is the simplest method, but it causes column obstruction and reduced recovery, sensitivity, and specificity of the analysis. However, direct injection of serum or samples was reported in some studies [34,35]. In order to control matrix effects, protein precipitation (PP), solid phase extraction (SPE), liquid-liquid extraction (LLE), and dispersive SPE (dSPE) have been used as common sample preparation techniques in most of the experiments [36–38]. Methanol, perchloric acid, acetonitrile, trichloroacetic acid, silver nitrate, and combination of H_2O with organic solvents followed by a fast centrifugation have been used to remove the proteins from biological samples. Among these compounds, silver nitrate exhibited an excellent effect on protein precipitation [39]. SPE, which is based

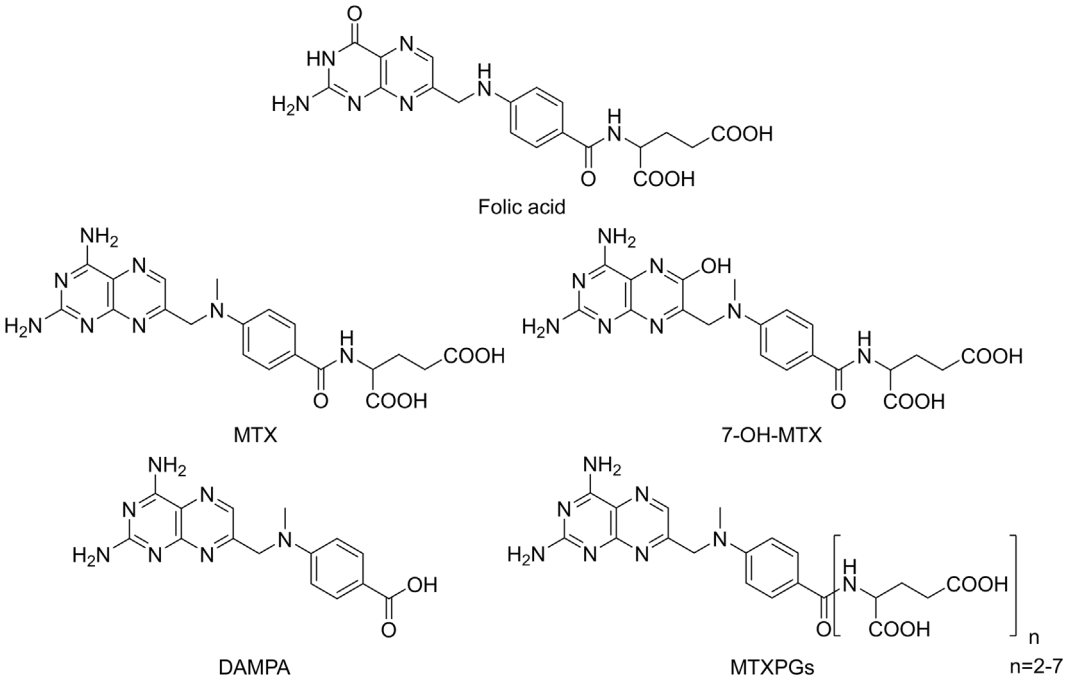

Fig. 1. Chemical structures of FA, and MTX and its main metabolites.

on the selective distribution of analytes between the solid and liquid phases, has been widely applied by different researchers [40–43]. For purification of samples with SPE, the sorbent (C_{18} as the common sorbent) that is inserted into syringes, disks, or cartridges, is influenced by vacuum pressure. Target components trapped in the solid phase and numerous volumes of solvents are used to eliminate sample matrix constituents. Finally, washing the purified analytes from solid phase is done with a suitable solvent. SPE can be performed either off-line or on-line. Off-line SPE is accomplished before instrumental technique, but on-line SPE is directly joined to the system. High sensitivity, low contamination, automation, and complete analysis can be obtained with the on-line method [44]. In the on-line SPE-LC, a pre-column, located in a six-port high-pressure switching valve is applied. Pre-concentration of sample is done on a pre-column during the injection and elution of analytes in the analytical column with valve switches [44]. As a selective separation method, Liu et al. used molecularly imprinted polymers (MIPs) as artificial recognition materials with extremely specific recognition properties along with SPE for the determination of MTX in human serum by HPLC. They used trimethoprim as a pseudo template for preconcentration, purification, and analysis of MTX in clinical samples to improve the method's sensitivity [40]. There are three imprinting methods for the application of MIPs in SPE to make a complex template-functional monomer: covalent imprinting, noncovalent imprinting, and hybridization of the two methods [45]. Both on-line and off-line SPE are applicable with MIP, but for the extraction of target substances in biological samples, the off-line type is usually used. High selectivity, stability, and a simple and inexpensive preparation can be obtained with MIPs [45]. The charged compounds in a solution can be extracted with ion exchange SPE. Liquid chromatography-strong anion exchanger (LC-SAX) and liquid chromatography-strong cation exchanger (LC-SCX) or liquid chromatography-weak cation exchanger (LC-WCX) bonded silica cartridges have been used for the separation of anionic and cationic materials, respectively [46]. The LC-SCX material comprises silica with aliphatic sulfonic acid groups that are bonded to the surface and used to extract strong cations, by ignoring recovery or elution. LC-WCX is applied for the recovery of a weak cationic species, which includes an aliphatic carboxylic acid group bonded to the silica surface [46]. SPE technique using a strong cation exchange (Bondesil SPE) was applied for MTX isolation [47]. The mentioned separation was carried out in the presence of formic acid and 5% ammonia in methanol as eluent. The electrostatic interaction of MTX charged carboxylate functional groups with the positively charged groups of the compound bonded to the silica surface is the basis of ion exchange SPE. LLE is based on mixing an immiscible solvent with an aqueous sample. After separating the phases, extraction of target analytes occurred through selective partitioning of the analytes and impurities between the phases [48]. Using large amounts of organic solvents with high purity, the need for solvent removal, and using evaporation are the disadvantages of LLE methods [49]. Microwave assisted extraction (MAE), as another preparation method for MTX, was also performed [50] for some environmental matrices. The extraction process was carried out using 25 mL of MeOH–H_2O (pH = 2) with a ratio of 1:1, heating at 110 °C in 10 min and then remaining at this temperature for another 30 min. MAE is based on microwave irradiation to heat the target and the extraction solvent. Quick preparation, low solvent consumption, high extraction efficiency, and ability to perform several simultaneous extractions are reached by MAE [51].

5. High performance liquid chromatography technique

By surveying the literature 2008–2019 it is revealed that HPLC equipped with UV–visible, fluorescence, and mass spectrometer detection has been the widely applied technique for the analysis of MTX and its metabolites, although fluorimetry, evaporative light scattering detector (ELSD), and electrochemical detection (ECD) might also be coupled with LC. The most frequently reported wavelength for HPLC-UV-visible detection is in the range of 302–400 nm in the case of 14 out of 24 evaluations and 5 out of 24 quantitation were performed under the wavelength of 300 nm. Three investigations were done by HPLC-fluorescent detection [37,52,53] and one measurement was by electrochemical detector [54]. Numerous stationary and mobile phases have been used in chromatographic methods; however, most of the HPLC experiments were done on C_{18} columns. LC techniques with pre-column or post-column derivatization were applied by some researchers. In pre-column derivatization, addition of reagents to the samples before the injection of samples to HPLC, but in the post-column method, addition of reagents to the elution takes place between the column and detector [55]. Post-column derivatization, as an automation and fast technique, occurs without introducing the reagents into the column. Thus, the chromatograms are bare of reagent and unreacted peaks. On the other hand, formation of the product in post-column derivatization occurs before detection, but in the case of pre-column derivatization, the stability of derivatized sample during the storing period and analysis is very important. In spite of the mentioned advantages of post-over pre-column derivatization, this technique also has some disadvantages including decreasing separation performance due to large reaction loops, requiring sophisticated apparatus, such as an additional pump and high amounts of reagents, and baseline variations [55]. Size exclusion chromatography (SEC), as a type of LC method, has been used for MTX determination [56]. The separation of biomolecules in SEC is based on the hydrodynamic radius. In this technique, molecules are eluted according to their molecular size, and the biomolecules are diffused in spherical porous particles of the stationary phase using an aqueous buffer as the mobile phase [57]. Since MTX polyglutamates (MTXPGs) aggregate in erythrocyte cells, a low cost and biocompatible measurement of all MTXPGs in erythrocyte cells can be accomplished by an HPLC equipped with fluorescence detection prior to post-column derivatization. The linearity range was 25–400 nmol/L [52]. Michaila et al. [58] applied SPE to separate MTX from indomethacin (IND) in human urine. Uchiyama et al. proposed a simple and sensitive HPLC method to determine MTX, 7-OH-MTX, and DAMPA in human plasma. Isocratic elution was performed on a Capcell Pak C_{18} UG120 (150 mm × 4.6 mm, 5 ìm) column using phosphate buffer (50 μmol/mL at pH 5.3) and acetonitrile (ACN) (9:1, v/v) as mobile phase at a flow rate of 0.5 mL/min, 5% aqueous ACN solution combined with 5% trichloroacetic acid was used to remove proteins from plasma. Fluorescent photolytic degradation products were produced by irradiation with UV light (245 nm) in a PTFE knitted capillary coil (3 m × 0.5 mm) inserted between the column and the detector. Excitation and emission wavelengths were at 368 and 425 nm, respectively. LOQ values for MTX, 7-OH-MTX, and DAMPA were 2.3, 0.38, and 3.4 ng/mL, respectively [37]. Begas et al. reported an HPLC method for MTX monitoring in osteosarcoma patients. Selectivity of the method was improved by using phenyl cartridges for SPE of MTX in human serum samples [59]. Determination of MTX, caffeine, diclofenac, glimepiride, and ibuprofen in the wastewater of Jordan was carried out by an HPLC/UV/fluorescence methodology. Chromatographic separation was accomplished with an RP-C_8 (250 mm × 4.6 mm, 5 μm) column using ACN and H_2O containing 0.1% trifluoroacetic acid with a ratio of 1:1 as mobile phase at flow-rate of 1 mL/min. UV detection was done at 225 nm to identify caffeine, nifidipen (internal standard), diclofenac, glimepiride, and ibuprofen. MTX detection was performed by the fluorescence

detector at $\lambda_{ex} = 367$ nm and $\lambda_{em} = 463$ nm. The limit of detections (LODs) and limit of quantifications (LOQs) were calculated as 0.9 and 3.0 μg/L for MTX, 0.6 and 1.9 μg/L for caffeine, 1.7 and 5.8 μg/L for diclofenac, 1.4 and 4.5 μg/L glimepiride, and 2.6 and 3.8 μg/L for ibuprofen, respectively [53]. Hu et al. reported an HPLC/UV method for the simultaneous quantification of carbamazepine, desipramine, guanabenz, MTX, propranolol, and warfarin with elution time of 6 min. The drugs were separated on a Agilent Zorbax SB-C_{18} (50 mm × 4.6 mm, 5 μm) column applying H_2O (containing 1% isopropyl alcohol and 0.01% heptafluorobutyric acid) as solvent A and ACN (containing 1% isopropyl alcohol and 0.01% heptafluorobutyric acid) as solvent B using gradient elution at a flow rate of 2.0 mL/min, and UV detection was performed at 280 nm. A linear range of 1.00–200 μM was obtained. LOD and LOQ were reported as 0.03 and 0.10 μM for carbamazepine, 0.10 and 0.30 μM for desipramine, 0.05 and 0.15 μM for guanabenz, 0.03 and 0.10 μM for MTX, 0.05 and 0.15 μM for propranolol, and 0.10 and 0.30 μM for warfarin, respectively. The optimized method was successfully applied to high throughput analysis for parallel artificial permeability assay [60]. A number of HPLC methods for the independent quantitation of IND [61–63], dexamethasone (DXM) [64,65] and MTX [66,67] were developed. Lariya et al. [68] determine MTX, DXM, and IND, simultaneously, by HPLC. Isocratic separation was done on a Luna C_{18} 100 R (250 mm × 4.6 mm, 5 μm) (Phenomenex, UK) column, with methanol and orthophosphoric acid at 70: 30 ratio as the mobile phase with a flow rate of 1.5 mL/min. The eluent was monitored via a photodiode array detector at 254 nm. The LOD and LOQ values were 3.3 and 10.9 ng for MTX, 0.3 and 0.9 ng for DXM, and 2.1 and 6.7 ng for IND, respectively. The linear range for all the analytes was 1–500 μg/mL [68]. A simple, but accurate analytical procedure for the simultaneous measurement of MTX and tretinoin in a pharmaceutical formulation was done by Agrawal et al. [69]. An HPLC apparatus equipped with UV–visible detector for the analysis of total MTX and SEC for the determination of free MTX were employed by Ciekot et al. in the macromolecular conjugates [56]. Quantitation of total MTX was done at the wavelength of 372 nm, with a linear range of 1.204–40.13 μM, LOD of 0.3150, and LOQ of 1.050 μM. The linear range, LOD, and LOQ of SEC were obtained as: 2.006–200.6 μM, 0.2761, and 0.9203 μM, respectively. Another study reported the simultaneous determination of MTX and FA in human plasma and urine of RA patients by means of ion chromatography equipped with electrochemical detector. To improve the detection sensitivity, glassy carbon electrode (GCE) was modified with quaternary amine functionalized multi-wall carbon nanotubes (q-MWNTs) [54]. Li et al. [39] determined the amount of MTX in human serum in the presence of silver nitrate 40% (w/v) which was used for serum protein precipitation. Wu et al. identified six impurities including N-methylfolic acid, 4-amino-N10-methylpteroic acid, N10-methylpteroic acid, MTX 5-methylester, MTX dimethyl ester, and for the first time, MTX 5-ethyl ester in a MTX drug product and quantified them by UPLC at the wavelength of 305 nm. DMSO was used to dissolve the MTX drug in order to reduce the hydrolysis of esterified impurities of MTX [70]. A robust HPLC technique by employing Quality by Design (QbD) for MTX evaluation in various forms such as tablet, injection, solid lipid nanoparticles (SLNs), SLN-gel, nanostructured lipid carriers (NLCs), NLC-gel, and lipid polymer hybrid nanoparticles (LPHNPs) was developed. Microemulsion, melt emulsification, and nanoprecipitation methods were used to prepare SLN, NLCs, and LPHNPs, respectively. Nanoprecipitation or solvent displacement method is based on the precipitation of a formed polymer from an organic solution and the transmission of the organic solvent in the aqueous phase in the existence or lack of a surfactant [71–75]. The emulsification method, as an improved type of solvent evaporation method [76], is based on the dissolution of encapsulating polymer in water soluble solvent, saturation with water, emulsification of polymer-water saturated solvent phase in an aqueous solution comprising stabilizer, and finally evaporation or filtration to remove the solvent, based on its boiling point. Preliminary screening was done using the Taguchi screening method to define the critical factors and to set their levels for the experimental design. Increasing the column life by means of decreasing the high concentration of buffer was the benefit of this method [77]. In another study, ionic gelation method was used for the synthesis of two kinds of nanogels loaded with MTX to investigate the neuropharmacokinetic effects of MTX. In this paper, the amounts of MTX in plasma, brain, and liver homogenates were determined by HPLC [78]. In ionic gelation method, two aqueous solutions consisting of a chitosan polymer and a polyanion sodium tripolyphosphate were used for the transition of the substances from liquid to gel medium because of the ionic interaction that causes the formation of ionic gelation [79]. Statistical calculations of MTX loaded on biodegradable microparticles with HPLC and UV–visible spectrophotometric techniques by Oliveira et al. showed that both methods provide similar results, and also can be used for the quality control of MTX in drug delivery systems [80]. Determination of MTX in rat plasma with HPLC-UV was done by Raichur and Devi [81]. The LOD and LOQ were 4 and 5 ng/mL, respectively. The method was also extrapolated to determine MTX in tablet formulation [81]. Similar measurement was performed by Roy et al. in bulk and tablet dosage forms. The retention time was 3.28 min and linearity was observed in the concentration range of 8–60 μg/mL [82]. Montemurro et al. optimized an HPLC-UV method for the therapeutic monitoring of MTX in plasma for patients with acute lymphoblastic leukemia (ALL). Utilizing core–shell particles, experimental design, and multiple response optimization enabled an analysis time of 4 min [38]. Although the analysis of MTX and metoclopramide (MCP) as an antiemetic agent was carried out separately, a new, quick, sensitive, and inexpensive method was designed for the simultaneous determination of MTX and MCP in bovine aqueous humor, vitreous humor, and human plasma by HPLC, for the first time [83]. The LODs of MTX for spiked plasma, spiked aqueous humor, and spiked vitreous humor samples were 18, 15, and 10 ng/mL, respectively; while, the LOQs were reported to be 25, 20 and 15 ng/mL, respectively. The proposed method was efficiently employed to determine MTX in polymeric nanoparticles. Instrumental conditions for the above-mentioned reports are presented in Table 1 [37–40,52–84,56,58–60,68–70,77–85].

6. Liquid chromatography-mass spectroscopy (LC–MS)

LC–MS has been definitely one of the best techniques for the analysis of anticancer drugs due to its low LODs. There are some limitations to adjust the flow rate and to apply the mobile phases in LC-MS. Usually, mixtures of H_2O and either methanol or acetonitrile are used as the mobile phase in RP-HPLC. In order to improve analyte separation, some common volatile additives, such as ammonium acetate, acetic acid, and formic acid, were used. Several ionization sources as the interface between the HPLC eluent and the mass spectrometer were utilized. Electrospray ionization (ESI) and atmospheric pressure chemical ionization (APCI) are the two most common ionization sources; however, the widely used ion source in the reviewed methods is ESI.

It is necessary to define the ions of mass formed in the ion source or viewed in a mass spectrum to fragment these ions and analyze the fragmentations [86]. Precursor ion, product ion, neutral loss, and selected reaction monitoring (SRM) are the four main scan modes of MS/MS, which provides more structural information on a selected ionic species. Multiple reaction mode (MRM) and SRM modes have been used to analyze MTX. For quantitative assays,

Table 1
High performance liquid chromatography parameters for the quantification of MTX and its metabolites.

Matrix	Analyte	Sample preparation	IS	Column	Mobile phase	Flow rate (mL/min)	Detector Temp. (°C)	Detector	LOD	LOQ	Linear range	Recovery (%)	Ref.
Human plasma	MTX	SPE	DAPA	C_{18} (150 mm × 4.6 mm, 5 μm)	90% PBS (50 μmol/mL, pH 5.3) and 10% ACN	0.5	15–20	Fuorescence detection at 368 [a]/425 [b]nm	11 pg	2.3 ng/mL	$r^2 = 0.999$	81.2–81.5	[37]
Plasma	MTX	Precipitation of proteins with ACN	Not used	C_{18} (3.0 mm × 75 mm, 2.7 μm)	HA/SAB (85.0 mM, pH 4.00) and 11.2% ACN	0.4	–	UV–visible at 305 nm	–	0.10 μM	0.10–6.0 μM	89.6	[38]
Human serum	MTX	Remove of proteins by SNS	Ferulic acid	C_{18} (250 mm × 4.6 mm, 5 μm)	78% SPB (10 mM, pH 6.40) and 22% MeOH	1.0	35	UV–visible at 310 nm	0.006 μg/mL	0.02 μg/mL	0.05–10.0 μg/mL	97.52	[39]
Human serum	MTX	SPE	Not used	C_{18} (250 mm × 4.6 mm, 5 μm)	23% MeOH and 77% aqueous solution of H_3PO_4 0.05%	1.0	–	UV–visible at 306 nm	–	–	–	81.6–86.2	[40]
RBC	MTX-Gls	Enzymatic treatment by PBS with MCE	Not used	C_{18} (250 mm × 4.6 mm, 5 μm)	11% ACN, 89% AAB (0.05 M, pH 5.5) and 0.25% H_2O_2 30%	0.6	–	fluorescence detection at 370 [a]/463 [b] nm	10.9 nmol/L	32.9 nmol/L	25–400 nmol/L	70.3–72.8	[52]
Waste water	MTX	SPE	Nifidipen	C_8 (250 mm × 4.6 mm, 5 μm)	50% ACN and 50% H_2O containing 0.1% TFA	1.0		Fluorescence detection at 367 [a]/463 [b]nm	0.9 μg/mL	3.0 μg/mL	$r^2 = 0.996$	92.3–110.5	[53]
Human plasma and urine samples	MTX	Remove of proteins by ACN and H_2O (1:1)	Not used	C_{18} (250 mm × 4.6 mm, 5 μm)	90% PBS (0.15 M, pH 5.0) and 10% ACN	1.0	–	Electrochemical	0.2 μg/L	–	0.01–20 mg/L	83–107	[54]
Macromolecular conjugates	MTX	Dissolvation of drug in SB	Not used	Superdex Peptide (150 mm × 4.6 mm, 5 μm)	0.1 M SB	0.4	22	UV–visible at 302 nm	0.2761 μM	0.9203 μM	1.204–40.13 μM	93.18–104.5	[56]
Urine	MTX	SPE	IBP	C_{18} (250 mm × 4.6 mm, 5 μm)	60% ACB (10 mM, pH 4) and 40% MeOH	1.5	–	UV–visible at 400 nm	0.03 μg/mL	0.08 μg/mL	0.08–10 μg/mL	84	[58]
Human serum	MTX	SPE	1,3,7-trimethyluric acid	C_{18} (250 mm × 4.6 mm, 5 μm)	89% SAB (50 mM, pH 3.6) and 11% ACN	1.0	30	UV–visible at 307 nm	0.003 μM	0.01 μM	0.025–5.00 μM	93.1–98.2	[59]
Drug	MTX	Dissolvation of drug in 5% DMSO (v/v) PBS	Not used	C_{18} (250 mm × 4.6 mm, 5 μm)	H_2O (including 1% isopropyl alcohol and 0.01% HFBA) and ACN (including 1% isopropyl alcohol and 0.01% HFBA)	2.0	20	UV–visible at 280 nm	0.03 μM	0.10 μM	1.00–200 μM	–	[60]
Drug	MTX	Dissolvation of drug in MP	IBP	C_8 (250 mm × 4.6 mm, 5 μm)	70% MeOH and 30% OPA (1.67%)	1.5	–	UV–visible at 254 nm	3.3 ng	10.9 ng	1–500 μg/mL	99.23–100.69	[68]
Pharmaceutical formulation	MTX	Dissolvation of drug in NaOH	Not used	C_{18} (250 mm × 4.6 mm, 5 μm)	85% ACN and 15% PBS	1.0	–	UV–visible at 340 nm	0.6 μg/mL	0.8 μg/mL	1–6 μg/mL	99–100.30	[69]
Drug	Impurities in MTX	Dissolvation of drug in DMSO	Not used	C_{18} (250 mm × 4.6 mm, 5 μm)	SDHP in water (20 mmol/L, pH 3.0) and ACN	2.2	40	UV–visible at 305 nm	<0.774 μg/mL	<1.03 μg/mL	$r^2 > 0.9999$	95.2–103 and 82.7–117 (at LOQ level)	[70]

(*continued on next page*)

Table 1 (*continued*)

Matrix	Analyte	Sample preparation	IS	Column	Mobile phase	Flow rate (mL/min)	Detector Temp. (°C)	Detector	LOD	LOQ	Linear range	Recovery (%)	Ref.
Tablets, injection, SLNs, SLN-gel and LPHNPs	MTX	Dissolvation of drug in NaOH	Not used	C_{18} (250 mm × 4.6 mm, 5 μm)	70% KH_2PO_4 buffer (10 mM, pH 3), 10% ACN and 20% MeOH	0.6	30	UV–visible at 302 nm	0.024 μg/mL	0.074 μg/mL	0.01–100 μg/mL	>95	[77]
Plasma, brain and liver	MTX	Dissolvation of drug in PTP 0.5% (w/v)	Not used	C_{18} (150 mm × 4.6 mm, 5 μm)	85% PBS (0.01 M, pH 3.9) and 15% ACN	1.0	–	UV–visible at 307 nm	–	–	–	–	[78]
Microparticles	MTX	Dissolvation of drug in an aqueous AA (1 wt%)	4-Amino AC	C_{18} (250 mm × 4.6 mm, 5 μm)	25% MeOH and 75% AAB (0.05 M, pH 6.0)	1.0	–	UV–visible at 303 nm	0.014 μg/mL	0.047 μg/mL	0.5–16 μg/mL	89.5–105.5	[80]
Plasma	MTX	Precipitation of proteins with ACN	Caffeine	C_{18} (250 mm × 4.6 mm, 5 μm)	89% PBS (0.01 M, pH 3.9) and 11% ACN	1.0	30	UV–visible at 303 nm	4 ng/mL	5 ng/mL	10–1000 ng/mL	93.02–96.93	[81]
Tablet	MTX	Dissolvation of drug in ACN	Not used	C_{18} (250 mm × 4.6 mm, 5 μm)	80% H_2O (pH 3 with HF) and 20% ACN	1.0	25	UV–visible at 211 nm	$0.0000279 \times 10^{-05}$ μg/mL	$0.0000847 \times 10^{-05}$ μg/mL	8–60 μg/mL	99.46–99.92	[82]
Physiological fluids	MTX	Precipitation of proteins with MeOH and PA	Sparfloxacin	C_{18} (250 mm × 4.6 mm, 5 μm)	36% MeOH and 64% TFA (0.05%)	1.0	40	UV–visible at 290 nm	Refer to text	Refer to text	0.025–1.0 μg/mL	98.57 (for plasma), 95.84 (for aqueous humor), 98.51 (for vitreous humor)	[83]
Polymeric nanocapsules	MTX	Dissolution of drug in MP	Not used	C_{18} (150 mm × 4.6 mm, 5 μm)	65% H_2O, 30% ACN, 5% THF (pH 3.0)	0.8	40	UV–visible at 313 nm	–	2.61μg/mL	10–50 μg/mL	96.74–101.23	[84]
Biopharmaceutical products	MTX	Dissolvation of yeastolate powders in H_2O	Not used	C_4 (250 mm × 4.6 mm, 5 μm)	0.05% TFA in water and 0.05% TFA in ACN	1.0	40	UV–visible at 302 nm	0.02 μM	0.09 μM	$r^2 > 0.9996$	97–105	[85]

IS: Internal standard, RBC: red blood cell, AAB: ammonium acetate buffer, ACB: acetate buffer, TEA: triethylamine, PBS: phosphate buffer solution, AA: acetic acid, ACN: acetonitrile, AA/SAB: acetic acid/sodium acetate buffer, SDHP: sodium dihydrogen phosphate, SPB: sodium phosphate buffer, HF: formic acid, THF: tetrahydrofuran, DAPA: 2,4-diaminopteroic acid, OPA: orthophosphoric acid, IBP: ibuprofen, TFA: trifluoroacetic acid, HFBA: heptafluorobutyric acid, 4-AminoAC: 4-aminoacetophenone, MCE: mercaptoethanol, MP: mobile phase, SB: sodium bicarbonate, SNS: silver nitrate solution, PTP: pentasodium triphosphate, PA: perchloric acid, MTX-Gls: MTX polyglutamates.

[a] Excitation.

[b] Emission.

SRM mode is used. Since the presence of the analyte in a sample is detected by measuring the *m/z* values of the predefined precursor and fragment ions, prior information on the fragmentation pattern of the sample in SRM mode is required [87]. Most studies on LC-MS/MS analysis of MTX and its metabolites are performed in MRM mode to identify and quantify the analytes by both its molecular ion and distinctive fragments. The highest sensitivity and specificity are obtained by MRM detection [48].

Due to high matrix effects in LC-MS, it is required to use suitable internal standards. MTX-d3 and aminopterin were reported to be used as the most common internal standard for LC-MS determination.

MTX detection in different samples such as RBCs [41], plasma [88], human saliva [89], and environmental samples [50] has been reported by LC-MS. Regarding the ability of LC-MS to detect impurities, as the most effective technique, Wu et al. [90] described a method for the simultaneous separation and identification of MTX impurities by LC-MS. Fifteen impurities, out of which ten were new compounds, identified in MTX drug substances by HPLC-PDA/FTICR-MS (High performance liquid chromatography joined with a photodiode array detector and Fourier transform ion cyclotron resonance mass spectrometry). In order to prevent esterified impurities, the researchers used DMSO as a solvent for the MTX drug product [90]. The MTX and $MTXPG_{2-7}$ measurement in human RBCs was accomplished by ion-pairing reversed-phase LC and electrospray ionization mass spectrometry and protein precipitation by perchloric acid. The LODs for individual MTXPGs were obtained 2.5 nM and 0.5 nM with 20 μL and 100 μL injection volumes, respectively. The separation of LC-PCR (hν, postcolumn photochemical reaction)–FD (fluorescent detection) was accomplished on a Phenomenex Intertsil C_{18} (150 mm × 4.6 mm, 5 μm) column. A fluorescence detector was used to detect compounds with excitation at 274 nm and emission at 470 nm. 10 mM sodium phosphate buffer pH = 6.2 with 1.5 mL/L 30% H_2O_2 as solvent A and 20% acetonitrile with 1.5 mL/L 30% H_2O_2 as solvent B were used as the mobile phase in gradient mode at a flow rate of 1.0 mL/min [41]. Previously, LC-PCR (hν)-FD was applied for the detection of MTXPGs by Dervieux et al., 2003 [91].

Simultaneous quantification of ten cytotoxic drugs including MTX, cytarabine (CYT), gemcitabine (GEM), etoposide phosphate, cyclophosphamide (CP), ifosfamide (IFO), irinotecan, doxorubicin, epirubicin, and vincristine was performed by LC–ESI–MS/MS method [92]. Analysis of the ten mentioned drugs on various surfaces such as stainless steel, polypropylene, polystyrol, glass, latex gloves, computer mouse, and coated paperboard were performed simultaneously, using wipe sampling procedure coupled with LC–MS/MS in SRM mode. The level of LOQs for all of the cytotoxic drugs was 0.1 ng/cm^2. The results were reported to be appropriate for environmental monitoring and to identify hospital personnel who were exposed to cytotoxic drugs [16]. Similar analysis was performed for simultaneous quantification of MTX, paclitaxel (PTX), CP, 5-fluorouracil (5-FU), vincristine (VNC), and oxaliplatin (OXP) with various physicochemical effects on stainless steel surface by Jeronimo et al. [93]. The data indicated that wiping procedures by trained staff compared to personnel without prior experience led to higher recovery. The LODs of MTX, PTX, CP, 5-FU, VNC, and OXP were reported to be 0.02, 0.01, 0.07, 4.66, 0.07, and 1.36 ng/mL, respectively.

Determination of whole-blood MTX and MTXPGs [94], quantitation of MTX and $MTXGlu_n$ ($n = 2–5$) in Caco-2 cells [95], analysis of $MTXPG_2$ to $MTXPG_7$ in patients with RA who receive low-dose oral methotrexate therapy [42] were performed using LC-MS.

Hawwa et al. described a selective and sensitive LC-MS-based methodology to determine MTXPGs in dried blood spots (DBS). Protein precipitation using perchloric acid followed by SPE was applied as the treatment procedure. It was shown that the developed method can be used for low volumes such as 12 μL in pediatric samples. A linear response was obtained in a range of 5–400 nmol/L. LODs and LOQs were 1.6 and 5 nmol/L for individual polyglutamates and 1.5 and 4.5 nmol/L for total polyglutamates, respectively. By comparing the data with conventional HPLC-UV, results showed a good correlation [43].

Simultaneous determination of MTX, dasatinib (DSN), and N-deshydroxyethyl dasatinib (M – 4) in Wistar rat plasma was performed by LC-MS/MS. MTX pharmacokinetic drug-drug interaction assay with DSN in rats after oral administration was evaluated with the mentioned method [88].

Rodin et al. performed a rapid and sensitive MTX quantitation in human saliva by SPE and LC–MS/MS technique. The method was linear in the concentration range of 2–2000 ng/mL and had a LOD value of 1 ng/mL. The authors successfully applied this method to a saliva excretion evaluation of MTX after an intravenous administration of 1 mg/kg of MTX to patients with acute lymphoblastic leukemia [89]. The quantitation of MTX in serum of rheumatic patients [96], estimation of MTX in human plasma [97], TDM of plasma MTX levels [98], and measuring of MTX in human plasma [99] are the additional studies using LC-MS.

Boer et al. developed a U–HPLC-ESI-MS/MS-based stable isotope dilution method to determine MTX in plasma without any special sample preparation. The analysis combined straightforward sample preparation, including dilution and protein precipitation, with a short (3-min) run time. Compared to traditional Abbott TDx fluorescent polarization immunoassay (FPIA) for MTX TDM, the presented methodology had an improved LLOQ (5 nM) and a large dynamic range (3–250 μM). Although this method exhibited a remarkable agreement when compared to the FPIA method, a small but significant negative constant error was identified. Consequently, it could be applied for routine clinical TDM [100]. UPLC or U-HPLC, referring to ultra-performance liquid chromatography, is an expanding chromatographic separation technique in which the particle size of stationary phase is smaller than 2.5 μm and the length of the columns is within 3–5 cm. These modifications improve peak resolution, speed, and sensitivity. Simultaneous determination of plasma MTX and 7-OH-MTX by UHPLC–MS/MS in patients receiving high-dose MTX therapy was done by Mei et al. [101]. The calibration range was 0.002–2 μM for MTX, and 0.01–10 μM for 7-OH-MTX. The LLOQ was 0.002μM for MTX and 0.01μM for 7-OH-MTX, respectively [101]. A generic UHPLC-MS method for the analysis of 24 antineoplastic drugs, including MTX, used in hospital pharmacy unit, with the help of a chromatographic modeling software, was developed by Guichard et al. The method was successfully applied for the analysis of pharmaceutical formulations and wiping samples from working environments [102].

A reliable analysis for a complex matrix such as RBCs can be obtained with stable-isotope-labelled internal standards. Application of stable-isotope-labelled internal standards for the analyses of $MTXPG_{1-5}$ in RBC with LC-MS/MS for the first time was performed by Boer and coworkers [103]. A pharmacokinetic survey of 5-FU in combination with low-dose MTX by LC-MS in mouse plasma, brain, and urine was reported [104]. LC-MS/MS technique was used for the simultaneous quantification of MTX and facitinib (TFB) in rat plasma, and it was shown that the validated evaluation was suitable for preclinical pharmacokinetic assays, pharmacokinetic–pharmacodynamic correlation, and toxicokinetic studies with an acceptable precision and accuracy [105]. For the first time, Schofield et al. reported rapid determination of MTX, 7-OH MTX, and 4-DAMPA in serum samples by turbulent flow liquid chromatography (TFC–LC) method coupled with electrospray positive ionization tandem mass spectrometry (TFC–LC–MS/MS).

The TFC is based on high mobile phase flow rates through large porous particles (30–60 μM). The small molecules are penetrated into the pores of the stationary phase, while larger molecules and matrix components are excluded, leading to waste. Then, by back-flushing with an organic solvent, the trapped molecules are desorbed from the TFC column and are inserted into the analytical LC–MS/MS system. Methanol, containing formic acid, was used for protein precipitation. HPLC separation was performed on Cyclone-P (50 mm × 0.5 mm) and Hypersil Gold C_8 (2.1 mm × 50 mm, 5 μm) columns. Water and methanol, each including 10 mM ammonium formate, were used as mobile phases A and B, respectively, at a flow rate of 0.7 mL/min. Acetonitrile: 2-propanol: acetone with a ratio of 6:3:1 (v/v/v) were selected as mobile phase C. TFC–LC separation was accomplished using mobile phases A, B, and C. The loading samples were prepared on the TFC in 100% mobile phase- A and were introduced into the liquid chromatography column with 80% mobile phase B. The authors claimed that the TFC–LC–MS/MS methodology is suitable for both routine clinical monitoring of MTX and the analytical determination of MTX after the administration of carboxypeptidase, as it is not affected by DAMPA [106]. High speed, reduced preparation of samples, as well as increased productivity and efficiency was obtained by TFC–LC–MS/MS [107].

An LC–MS/MS methodology for the simultaneous determination of MTX, 6-mercaptopurine (MP), and its metabolite 6-thioguanine (TG) in plasma of children with acute lymphoblastic leukemia was developed. A good extraction recovery was obtained by SPE using a strong cation exchanger. The comparison of fresh samples and stock solutions of MTX, MP and TG kept for 15 h at temperature of 2–8 °C confirmed adequate stability of the stock solutions [47]. On-line SPE coupled with reversed-phase liquid chromatography-switching polarity electrospray ionization-tandem mass spectrometry (LC-ESI (±)-MS/MS) was applied for quantitation of the trace amounts of bezafibrate, MTX, CP, orlistat, and enalapril in waste and surface waters by Garcia-Ac et al. The LOD and LOQ for the compounds in MQ water, wastewater effluent and influent, and surface water were in the low ng/L range and the method intra-day precision was less than 6.5% [108]. Moreover, the analysis of contaminants in liquid and solid environmental samples such as crude wastewater, final effluent, and river water by ultra-HPLC-MS were reported by Petrie et al. [50]. Separation of acidic compounds such as non-steroidal anti-inflammatory drugs (NSAIDs), steroid estrogens, parabens, and some benzophenones in the environmental samples were performed using H_2O (80%) and MeOH (20%) containing 1 mM NH_4F as the mobile phase A and H_2O (5%) and MeOH (95%) also containing 1 mM NH_4F as the mobile phase B. The separation conditions of basic compounds were NH_4OAc 5 mM in H_2O (80%), and MeOH (20%) containing 0.3% CH_3COOH as the mobile phase A and MeOH as mobile phase B. In both methods, EH C_{18} (150 mm × 1.0 mm, 1.7 μm) was chosen as the column. MAE process was chosen to extract solid matrices. Quick preparation, decreased solvent consumption, and performing several extractions at the same time were reached using MAE. Another report about hazardous antineoplastic drugs is the determination of CP, IFO, and MTX by ESI-LC–MS/MS as a highly sensitive, specific, and reliable method to monitor the urine of employees, occupationally exposed to antineoplastic drugs [109]. HPLC coupled with HRMS (high resolution mass spectrometry) was selected to analyze 5-FU, carboplatin (C–Pt), CP, CYT, DOX, GEM, IFO, MTX, and mitomycin C (MIT) in numerous hospital environment sites without derivatization and complex extraction procedures for polar compounds [110]. The quantitation of MTX and 7-OH-MTX in human urine was performed by Bluett et al. using LC-MS adjusted in SRM mode. To improve specificity and diminish cross-reaction, determination of MTX and 7-OH-MTX in the urine was done for up to 105 and 98h after drug administration, respectively [111]. Instrumental parameters for the above-mentioned methods are described in Table 2 and Table 3.

7. Mass spectrometry

Roland et al. proposed a method to determine MTX and MTXPGs in erythrocyte lysates by ultrafast matrix-assisted laser desorption/ionization (MALDI) and triple quadrupole (tandem) mass spectrometry (MALDI-QqQ-MS/MS). The procedure involved SPE of MTX and MTX-MTXPG metabolites from deproteinized erythrocyte lysates using aminopterin as the internal standard. The LLOQ and LOD were 10 and 0.3 nmol/L, respectively. The method was used to find MTX and MTX-MTXPG metabolites concentrations in patients with RA who had received low-dose oral MTX therapy. The authors declared that elimination of LC in combination with MALDI, reduced analysis time: therefore, this method is applicable for high-throughput measurements of large number of samples [42]. $MTXPG_5$ was detected as the highest glutamylation. $MTXPG_6$ and $MTXPG_7$ were not identified in the erythrocyte pellets of RA patients.

8. Capillary electrophoresis (CE)

CE is applied to separate charged analytes and is based on the difference in electrophoretic mobilities of ions, leading to various migration rates [112]. Direct injection of biological fluids to CE is possible when the drug concentration is at amounts higher than mg/L or g/L [113,114]. Due to the lower amount of sample volume and smaller cell path detection in CE compared with HPLC, CE equipped with UV detector is not sensitive enough to measure drugs in mg scale. Therefore, increasing the amount of injected samples to capillary column and modifying the detector sensitivity are applied to enhance the sensitivity of CE [113].

CE using low amount of sample, cheap capillaries, high speed, and high resolution and efficiency has been proposed as another technique to separate MTX in different matrices, by Castro-Puyana et al., Cheng et al., and Guichard et al. [115–118]. Due to the importance of cerebrospinal fluid (CSF) during chemotherapy and relapse, the evaluation of MTX and its metabolites in CSF was performed by triple-stacking CE [116]. In this report, due to the low charge of sample ions, samples were injected hydrodynamically. UV–visible detection is a common detector in CE; however, it is not suitable for identification of enantiomeric impurities in biomedical samples. Therefore, electrokinetic chromatography (EKC) as a type of CE with luminescence detection was used to separate chiral MTX [115]. In addition, amperometric biosensors [119], voltammetric methods [120], potentiometric membrane electrodes [121], TLC [122], HPLC [123], and CE [124–126] were also reported to be used for chiral determination of MTX. The instrumental parameters for CE detection of MTX are described in Table 4.

9. UV–visible spectrophotometry

As the heteroaromatic pterin chromophore [127] in the structure of MTX causes the molecule to strongly absorb UV–visible, it is possible to assay the amount of MTX by the low cost UV–visible spectrophotometry. At neutral pH, the pterin chromophore shows the maximum molar extinction, whereas at acidic pH a reduction of absorbance occurs [127]. Moreover, it is possible to obtain the first or higher order derivatives of absorbance against wavelength by UV–visible spectrophotometry to identify the overlapped spectra, especially in pharmaceutical analysis [128]. Researchers performed the analysis with zero-order derivatization or area under the curve measurement (AUC method). Zero-order derivatization is performed in a single wavelength, but the AUC method is performed

Table 2
Liquid chromatographic and MS conditions of LC-MS methods for MTX and its metabolites quantification.

Sample	Preparation	LC conditions	Interface	Target analyte	*m/z* of mass transition	IS	LOD[a]	LOQ[a]	Recovery (%)	Ref.
Different surfaces	Whatman filter paper	C_{18} (2.1 mm × 100 mm, 3.5 μm) column. H_2O, ACN and HF 1% as mobile phase at a flow rate of 200 μL/min.	ESI/SRM$^+$	CYT, GEM, MTX, [^{13}C,$^2H_3$] MTX, Et Ph, IFO, CP, IRI, DOX, EPI, VNC	244.0 > 112.3, 264.7 > 112.3, 455.2 > 308.4, 459.2> 312.2, 691.0 > 691.0, (261.1 > 92.3, 140.2, 154.1, 232.9), (261.1 > 92.3, 140.2, 154.1, 232.9), 587.9 > 587.3, (544.6 > 379.2, 397.1), (544.6 > 379.2, 397.1), 413.3 > 353.2	[^{13}C,$^2H_3$] MTX	0.1−1 pg/sample	0.1 ng/cm^2	99	[16]
RBCs	SPE	C_{18} (50 mm × 1.00 mm, 4 μm) column. NH_4HCO_3 (10 mM, pH 7.5) with 5 mM DMHA, ACN with 5 mM DMHA as mobile phase at a flow rate of 200 μL/min	ESI/MRM$^+$	MTXPG1, MTXPG2, MTXPG3, MTXPG4, MTXPG5, MTXPG6, MTXPG7	455.2 > 308.1, 584.3 > 308.1, 713.3 > 308.1, 842.3 > 308.1, 971.3 > 308.1, 1100.4 > 308.1, 1229.4 > 308.1	Aminopterin	0.8 nM	2.5 nM	31.2−47.8	[41]
Human erythrocyte	SPE	Not used	MALDI/SRM$^+$	MTX, MTXPG2, MTXPG3, MTXPG4, MTXPG5, MTXPG6, MTXPG7, Aminopterin	455.2 > 308.2, 584.4 > 308.2, 713.4 > 308.2, 842.4 > 308.2, 971.6 > 308.2, 1100.3 > 308.2, 1229.4 > 308.2, 441.2 > 294.2	Aminopterin	1 nmol/L	10 nmol/L	62.4−71.3	[42]
DBS	SPE	C_{18} (150 mm × 2.1 mm, 3 μm) column. ABB (10 mM, pH 7.5) and ACN as mobile phase with flow rate of 0.15 mL/min	ESI/MRM$^+$	MTXPG1, MTXPG2, MTXPG3, MTXPG4, MTXPG5	455.40 > 175.05, 584.40 > 175.05, 713.40 > 175.05, 842.30 > 175.05, 971.60 > 175.05	Not used	1.6[b] nM, 1.5[c] nM	5[b] nM, 4.5[c] nM	44−72	[43]
Plasma	SPE	Acquity UPLC BEH shield RP (2.1 mm × 150 mm, 1.7 μm) column, 85% ACN and 15% aqueous HF (0.1%) as mobile phase at 40 °C and flow rate of 0.8 mL/min	ESI/MRM$^+$	MTX, MP, TG, TU	455.34 > 308.22, 152.89 > 119.00, 168.01 > 151.08, 128.94 > 111.90	TU	–	–	94.28−102.22	[47]
ECs in liquid and solid environmental matrices	MAE	Refer to text	ESI/MRM^{+a}	–	–	ACE-D4, IBP-D3, BIS A-D16, CAR-13C6, KET-D3, NAP-D3, SER-D3, TAM, ATE-D5 13C2, PRO-D7 15 N, MET-D6, BEZ-D6, MET-13C, AMP-D5, MET-D5, MDMA-D5, MDA-D5, Heroin-D9, codeine-D6, ketamine-D4, cocaine-D3, BEN-D8, EDDP-D3, MOR-D3, COT-D3, COCA-D8, TEM-D5, 1S,2R-(+) ephedrine-D3, MEPH-D3, METH-D9, NOR-D4, estrone (2,4,16,16-D4), estradiol (2,4,16,16-D4), QUE-D8 HEM, CIS-D6, MET-D7, FLU-D5, MIR-D3	6.13−9.04 ng/L and 1.64 ng/g	20.24−29.83 ng/L and 5.42 ng/g	40−152	[50]

(*continued on next page*)

Table 2 (*continued*)

Sample	Preparation	LC conditions	Interface	Target analyte	*m/z* of mass transition	IS	LOD[a]	LOQ[a]	Recovery (%)	Ref.
Plasma	LLE	C_{18} (50 mm × 3 mm, 4.6 μm) column. MeOH, AAB (2 mM, pH 4.0) as mobile phase at a flow rate of 1 mL/min	HESI/SR$^+$	MTX, DSN, M-4, TOL	455.0 > 175.0, 488.1 > 401.0, 444.26 > 401.0, 271.1 > 155.0	Tolbutamide	–	1 ng/mL	79.4–87.2[a]	[88]
Human saliva	SPE	C_{18} (150 mm × 2 mm, 2.2 μm) column, 0.1% HF and ACN as mobile phase at a flow rate of 0.4 mL/min	ESI/MRM$^+$	MTX, Aminopterin	455.6 > 308.4, 441.2 > 294.0	Aminopterin	1 ng/mL	–	89–94	[89]
Drug	Dissolvation of drug in DMSO	C_{18} (250 mm × 4.6 mm, 5 μm) column, 0.2% HF and ACN as mobile phase at a flow rate of 1 mL/min	ESI$^+$	$C_{19}H_{21}N_8O_5^+$, $C_{20}H_{23}N_8O_6^+$, $C_{20}H_{23}N_8O_6^+$, $C_{15}H_{17}N_8O^+$, $C_{20}H_{22}N_7O_6^+$, $C_{19}H_{21}N_8O_5^+$, $C_{20}H_{23}N_8O_6^+$, $C_{22}H_{27}N_8O_6^+$, $C_{19}H_{21}N_8O_4^+$, $C_{15}H_{16}N_7O_2^+$, $C_{21}H_{25}N_8O_5^+$, $C_{18}H_{19}N_8O_3^+$, $C_{22}H_{27}N_8O_5^+$, $C_{22}H_{27}N_8O_5^+$, $C_{22}H_{27}N_8O_5^+$, $C_{15}H_{15}N_6O_3^+$	(441.16278 > 441, 294), (71.17325 > 471, 308), (471.17319 > 471, 308), (325.15192 > 305, 308), (456.16232 > 456, 309), (441.16269 > 441, 308), (471.17343 > 471, 324), (499.20453 > 499, 308), (425.16794 > 425, 308), (326.13599 > 326, 175), (469.19379 > 469, 308), (395.15720 > 395, 308), (483.20950 > 483, 308), (483.20947 > 483, 308), (483.20953 > 483, 308), (327.11975 > 327, 309)	Not used	–	–	–	[90]
Pharmaceutical formulations and wipe samples	Dilution with H_2O	C_{18} (2.1 mm × 100 mm, 3.5 μm) column at 15 C. H_2O, ACN and HF 1% as mobile phase at a flow rate of 200 μL/min	ESI/SRM$^+$	CYT, GEM, MTX, [^{13}C,$^2H_3$] MTX, Et Ph, IFO, CP, IRI, DOX, EPI, VNC	244.0 > 112.3, 264.7 > 112.3, 455.2 > 308.0, 459.2 > 312.2, 691.0 > 691.0, (261.1 > 92.3, 140.2, 154.1, 232.9), (261.1 > 92.3, 140.2, 154.1, 232.9), 587.9 > 587.3, 544.6 > 379.2, 397.1), (544.6 > 379.2, 397.1), 413.3 > 353.2	[^{13}C,$^2H_3$] MTX	0.01 ng/mL	0.25 ng/mL	85–110	[92]
Stainless steel surface	Whatman filter paper wetted with 20% H_2O and 80% MeOH with 0.1% HF	Biphenyl (50 mm × 4.6 mm) column. H_2O (pH 2.3 adjusted with HF-AF) and MeOH as mobile phase at a flow rate of 0.6 mL/min	ESI/MRM$^+$	5- FU, OXP, CP, PTX, VNC, MTX	131 > 114, 398 > 306, 261 > 141, 876.3 > 308.1, 825.6 > 765.6, 455.2 > 308.1	MTX-methyl-d_3, paclitaxel-d_5, vincristine-d_3 sulfate, cyclophosphamide-d_4	0.02 ng/mL	0.06 ng/mL	102[a]	[93]
Human whole blood	Precipitation with 50% trifluoroacetic acid, and extraction by EtOAc	C_{18} (2.1 mm × 100 mm, 3 μm) column. 70% AF (20 mM) and 30% ACN (1% HF) as mobile phase at room temperature and flow rate of 0.2 mL/min	ESI/MRM$^+$	MTX, Doxofylline	455.2 > 308.2, 267.2 > 181.2	Doxofylline	0.5 ng/mL	1 ng/mL	26.2–37.8	[94]
Caco-2 cells	Protein precipitation by ice-cold ACN	C_8 (150 mm × 3.9 mm, 5 μm) column. 0.1% HF and ACN as mobile phase at flow rate of 0.5 mL/min	ESI/MRM$^+$	MTX, MTX-Glu_2, MTX-Glu_3, MTX-Glu_4, MTX-Glu_5, Aminopterin	455.2 > 308.2, 584.1 > 308.2, 713.1 > 308.2, 842.1 > 308.2, 971.1 > 308.2, 441.3 > 294.2	Aminopterin	–	2 nM	60-79[a]	[95]
Serum	Protein precipitation by MeOH.	C_{18} (100 mm × 4.6 mm, 3 μm) column. 88% AA 1%	ESI/MRM$^+$	MTX	455.2 > 308.1	Pterin	3.0 nM	10.0 nM	100.4	[96]

		and 12% ACN as mobile phase at a flow rate of 0.5 mL/min								
Human plasma	SPE	(50 mm × 4.6 mm, 5 μm) column. 70% ACN, 15% AF (10 mM) and 15% HF (0.5%) as mobile phase at 40 °C and flow rate of 0.6 mL/min	ESI/MRM$^+$	MTX, MTX-d_3	455.3 > 308.2, 458.3 > 311.2	MTX-d_3	–	0.500 ng/mL	85.6	[97]
Plasma	Protein precipitation by 70% ACN and 30% H_2O	C_{18} (50 mm × 2.1 mm, 3 μm) column. 0.03% AA and ACN as mobile phase at a flow rate of 0.5 mL/min	ESI/MRM$^+$	MTX, *p*−amino ACP	455.3 > 308.3, 136.1 > 94.4	p−amino ACP	–	0.05 μmol/L	>94	[99]
Plasma	Protein precipitation by addition of 800 μL of cold 16% perchloric acid	C_{18} (2.1 mm × 100 mm, 1.7 μm) column, 21% CH_3OH and 79% ABC (10 mM, pH 10) with a flow rate of 0.3 mL/min	ESI/SRM$^+$	MTX, MTXd$_3$	455.2 > 308.2, 458.2 > 311.2	MTX-d_3	–	5 nM	96−102	[100]
Plasma	Protein precipitation with MeOH	C_{18} (2.1 mm × 50 mm, 1.7 μm) column at 37 °C. MeOH (0.1% HF) and H_2O (0.1% HF) as mobile phase with a flow rate of 0.4 mL/min	ESI/MRM$^+$	MTX, 7-OH-MTX, MTX-d_3	455.2 > 308.2, 471.2 > 324.1, 458.2 > 311.2	MTX-d_3	–	0.002 μM	88.6−92.6	[101]
Drug	Dilution with DMSO	CORTECS® T3 (100 mm × 2.1 mm, 1.6 μm) column at 25 °C. 10 mM AA (pH 5.1) and ACN as mobile phase with a flow rate of 0.4 mL/min	ESI$^+$	MTX	459.2 > 454.4	–	–	–	–	[102]
RBCs	Protein precipitation by adding cold 16% perchloric acid	C_{18} (2.1 mm × 100 mm, 1.7 μm) column at 35 °C. ABC (10 mM, pH 10) and MeOH as mobile phase at flow rate of 0.3 mL/min	ESI/SRM$^+$	MTXPG1, MTXPG2, MTXPG3, MTXPG4, MTXPG5	455.2 > 308.2, 584.4 > 308.2, 713.4 > 308.2, 842.4 > 308.2, 971.6 > 308.2	Stable-isotope labelled	–	1 nM	54−98	[103]
Plasma, brain and urine	Protein precipitation with MeOH and ACN	C_{18} (150 mm × 3 mm, 3.5 μm) column. 70% AA (5 mM) and 30% MeOH as mobile phase with flow rate of 300 μL/min	For MTX and AMP: ESI/SRM$^+$, for 5-FU and 5-BU: ESI/SRM$^-$	–	–	5-BU[a]	–	15.6 ng/mL (plasma and brain), 78.1 ng/mL (urine)	24.1−58.1	[104]
Plasma	SPE	C_{18e} (100 mm × 4.6 mm) column. 25% AA (5 mM, pH 5.0) and 75% ACN as mobile phase with a flow-rate of 0.4−0.8 mL/min	ESI/MRM$^+$	MTX, TFB, Phenacetin	455.2 > 308.3, 313.2 > 149.2, 180.3 > 110.2	Phenacetin	–	0.49 ng/mL	84.8−90.7	[105]
Serum	Protein precipitation by MeOH containing HF	Refer to text	ESI/SRM$^+$	MTX, 7-OH MTX, DAMPA, MTX-d_3	455.1 > 308.1, 471.2 > 324.2, 326.1 > 175.1, 458.1 > 311.1	MTX-d_3	–	10 nmol/L	92.4−107.4	[106]
WWTP	On-line SPE	C_{18}	ESI/SRM$^-$: BEZ, other analytes: ESI/SRM$^+$	CP, BEZ, ENA, MTX, OR	261.0 > 140.0, 360.1 > 273.9, 377.2 > 234.1, 455.1 > 308.0, 496.4 > 319.2	Not used	6−16 ng/L	19−47 ng/L	55-125[a]	[108]

(*continued on next page*)

Table 2 (*continued*)

Sample	Preparation	LC conditions	Interface	Target analyte	*m/z* of mass transition	IS	LOD[a]	LOQ[a]	Recovery (%)	Ref.
Urine	SPE	C_{18} (100 mm × 2.1 mm, 5 μm) column at 20 °C. AF (4 mM, pH 3.2), ACN as mobile phase with a flow rate of 0.3 mL/min	ESI/MRM$^+$	MTX, MTX-d_3, CP, IF, CP-d_4	455.10 > 308.2, 455.10 > 311.20, 261.08 > 140, 261.08 > 92, 264.90 > 140	CP-d_4 and MTX-d_3	10 pg/mL	20 pg/mL	78.3[a]	[109]
Hospital environment sites	Washing wipes with suitable solvents	C_{18} (150 mm × 2 mm, 3 μm) column. 0.05% HF and MeOH as mobile phase at flow rate of 200 μL/min	ESI/MRM$^-$: 5-FU, other compounds: ESI/MRM$^+$	5-FU, C-Pt, CYC, CYT, DOX, GEM, IFO, MTX, MIT	129.0095 > 85.0033 , 372.0518> 355.0252, 261.0321 > 140.0028, 244.0928 > 112.0505, 544.1813 > 397.0918, 264.0790 > 112.0505, 261.0321 > 182.0132, 455.1786 > 308.1254, 335.1350 > 242.0924	Not used	–	1ng/mL	87.2[a]	[110]
Urine	Protein precipitation by ACN	Hypersil GOLD™ (100 mm × 2.1 mm, 1.9 μm) column at 25 °C. 0.1% HF and ACN with 0.1% HF as mobile phase at a flow rate of 0.3 mL/min	ESI/SRM$^+$	MTX, 7-OH-MTX, MTX-d_3	455.1 > 308.1, 471.1 > 324.1, 458.1 > 311.1	MTX-d_3	–	2.5 nM	104- 126[a]	[111]

IS: Internal standard, LC: liquid chromatography, ACN: acetonitrile, HF: formic acid, TU: thiouracil, SPE: solid phase extraction, MAE: microwave assisted extraction, EtOAc: ethyl acetoacetate, p −amino ACP: p-amino-acetophenone, ECs: emerging contaminants, ACE-D4: acetaminophen-D4, IBP-D3: ibuprofen-D3, BIS A-D16: bisphenol A-D16, CAR-13C6: carbamazepine-13C6, KET-D3: ketoprofen-D3, NAP-D3: naproxen-D3, SER-D3: sertraline-D3, TAM 13C2 15N: tamoxifen 13C2 15N, PRO-D7: propranolol-D7, ATE-D5: atenolol-D5, MET-D6: metformin (dimethyl-D6), BEZ-D6: Bezafibrate-D6, MET-13C: Methylparaben-13C, AMP-D5: amphetamine-D5, MET-D5: methamphetamine-D5, codeine-D6, ketamine-D4, cocaine-D3, BEN-D8: benzoylecgonine-D8, EDDP-D3, MOR-D3: morphine-D3, COT-D3: cotinine-D3, COCA-D8: cocaethylene-D8, TEM-D5: temazepam-D5, 1S,2R-(+) ephedrine-D3, MEPH-D3: mephedrone-D3, METH-D9: methadone-D9, NOR-D4: norketamine-D4, estrone (2,4,16,16-D4), estradiol (2,4,16,16-D4), QUE-D8 HEM: quetiapine-D8 hemifumurate, CIS-D6: citalopram-D6, MET-D7: metoprolol-D7, FLU-D5: fluoxetine-D5, MIR-D3: mirtazapine-D3, AF: ammonium formate, MALDI: matrix-assisted laser desorption ionization, a: (+)-MTX, b: (-)-MTX, DMHA: dimethylhexylamine, RBCs: red blood cells, CP-d4: cyclophosphamide-d4, MTX-d3: methotrexate-d3, AA: acetic acid, 5-FU: 5-fluorouracil, C-Pt: carboplatin, CYC: cyclophosphamide, CYT: cytarabine, DOX: doxorubicin, GEM: gemcitabine, IFO: ifosfamide, MIT: mitomycin C, WWTP: wastewater treatment plants, BEZ: bezafibrate, CP: cyclophosphamide, OR: orlistat, ENA: enalapril, ABC: ammonium bicarbonate, TFB: tofacitinib, DBS: dried blood spots, ABB: NH4HCO3 buffer, OXP: oxaliplatin, PTX: paclitaxel, VNC: vincristine, Et Ph: Etoposide phosphate, IRI: Irinotecan, EPI: Epirubicin, LLE: liquid-liquid extraction, AAB: ammonium acetate buffer, DSN: Dasatinib, M-4: N-deshydroxyethyl dasatinib, TOL: tolbutamide, HESI: heated electron spray ionization, 5-BU: 5-bromouracil.

[a] Only for MTX.

[b] For individual MTXPGs.

[c] For $MTXPG_{total}$.

Table 3
Mass spectrometric parameters of LC-MS methods for MTX and its metabolites quantification.

Analyte	Ion source temperature (°C)	ISV	Collision gas/pressure (psi)	NEB gas/pressure (psi)	AUX gas/pressure (psi)	CE	Linear range	Ref.
MTX	325	4 kV	Ar	–	N_2	20 eV	–	[16]
MTX	125	3.0 kV	Ar	–	–	20 V	0.5–100 nM	[41]
MTX	–	–	N_2	–	–	25 V	–	[42]
$MTXPG_n$	135	–	–	N_2	–	36–67V	5–400 nmol/L	[43]
MTX	–	–	–	–	–	20 V	6.25–200.00 ng/mL	[47]
MTX	350	4500 V	Ar	–	N_2	3500 eV	0.97–931.37 ng/mL	[88]
MTX	300	5500 V	N_2/15	N_2/30	–	23 V	2–2000 ng/mL	[89]
Impurities in MTX	275	35 V	He	N_2	–	35%	–	[90]
MTX	325	4 kV	Ar	–	N_2	20 eV	1–200 ng/mL	[92]
MTX	–	4000 V	N_2	N_2/40	–	16 V	r^2: 0.9980[a]	[94]
MTX	400	5.5 kV	N_2/12	N_2/60	N_2/50	35 V	2–250 nM	[95]
MTX	100	1 kV	–	–	–	16 eV	10–1000 nM	[96]
MTX	500	5500 V	–	–	–	28 eV	22.7–11360 ng/mL	[97]
MTX	400	4500 V	–	35	–	23 V	0.05–100 μmol/L	[99]
MTX	120	–	Ar	–	–	20 eV	Up to 50 μM	[100]
MTX	550	5500 V	–	–	–	26 V	0.002–2 μM	[101]
MTX	150	3 kV	–	–	–	–	–	[102]
$MTXPG_n$	–	–	Ar	–	–	20, 40 & 50 eV	1–1000 nM	[103]
MTX	–	5000 V	–	–	–	31 V	0.49–91.0 ng/mL	[105]
MTX	–	4500 V	Ar	–	N_2/15	–	10–1000 nmol/L	[106]
MTX	350	3.5 kV	Ar	–	N_2	21 V	–	[108]
MTX	120	1.5 kV	Ar	–	–	26 eV	250–1250 pg/mL	[109]
MTX	–	–	–	–	N_2	35 V	r^2: 0.983	[110]
MTX	350	4000 V	N_2	–	–	25 eV	r^2: 0.9977	[111]

ISV: Ion spray voltage, CE: collision energy, NEB: nebulizing, AUX: auxiliary.
[a] For whole blood.

between two selected wavelengths. Consequently, lower LODs and LOQs were obtained with AUC method [129–133]. Only recently, Hamidi et al. proposed a novel mixed hemimicelles dispersive micro-SPE using ionic liquid functionalized magnetic graphene oxide/polypyrrole for the extraction and pre-concentration of MTX from urine samples of patients with acute lymphoblastic leukemia under MTX therapy, receiving an intravenous dose of 1 mg/kg of MTX. The extracted analyte was quantified by a UV–visible spectrophotometer and the accuracy of the method was confirmed by HPLC measurements. A linear range of 10–1000 ng/mL with a good correlation ($r^2 = 0.99$) was obtained and the LOD was reported to be 7 ng/mL. As the authors claimed, the sensitivity was superior to or comparable with that of other methods, especially those coupled with sophisticated detectors. Less sample treatment time, reduced use of hazardous and water-immiscible solvents and minimal transferring steps were among the highlighted points in this methodology [134]. The instrumental conditions for the UV–visible spectrophotometric MTX detection are described in Table 4.

10. Electrochemical methods

Among the analytical techniques for quantitation of MTX, electrochemical methods could be an appropriate choice due to simple, inexpensive, and fast procedure without having tedious sample preparation [135]. Reduction reaction of MTX in neutral and acidic solutions is a three-step process with two-electron/two-proton transmissions [136]. In the first step, 5, 8-dihydro-MTX is formed, which tautomerizes to 7, 8-dihydro-MTX. The C(9)–N(10) bond of 7, 8-dihydro-MTX is separated in the next step; and finally, petridine is converted into its 5, 6, 7, 8-tetrahydro derivative. Reduction of MTX in alkaline solutions is a single step with two-electron/two-proton transmissions, which is the result of a very slow tautomerization step, so to create the reactant for subsequent reductions [136]. Hanging mercury drop electrode (HMDE) or static mercury drop electrode (SMDE) with cyclic voltammetry (CV) and differential pulse voltammetry (DPV) or adsorptive stripping differential pulse voltammetry (AdSDPV) have been used for the analysis of MTX by electrochemical methods [135]. Recently, modified electrodes with nanoparticles which reduce the overpotential and increase the reaction rate of many electroactive substrates have been used by different researchers [137,138]. Carbon nanotubes, gold and silver nanoparticles have created promising horizons for sensing systems [139]. Modification of a glassy carbon electrode (GCE) with multiwalled carbon nanotubes functionalized with quaternary amine (q-MWCNTs) [140], modification of GCE with MWCNTs immobilized within a dihexadecylhydrogenphosphate film as a nanostructured patent [138], modification of GCE with DNA functionalized single-walled carbon nanotube (DNA/SWCNT), and nafion composite film [141] for MTX quantification have been reported in recent studies. Detection limits at nanomolar (nM) range were obtained in some of the investigations. For example, modification of GCE with $CoFe_2O_4$/reduced graphene oxide (rGO) and ionic liquid in phosphate buffer solution (PBS) at pH 2.5 [142], modification of GCE with poly L-lysine in the presence of sodiumdodecyl benzene sulfonate (SDBS) [143], AdSDPV technique along with a bismuth film electrode (BiFE) [144], synthesized nanocomposites of N–graphene coated with a bimetallic palladium-silver alloy (PdAg/NG–GCE) [145], 3D porous graphene-carbon nanotube (G-CNT) network on the surface of GCE [146], modification of GCE with cyclodextrin-graphene hybrid nanosheets [147] achieved LODs in the range of 0.01–70 nM. Studies reporting electrochemical methods are listed in Table 4 [148–153].

11. Nanomaterial optical probes

Nanomaterials have revealed their appropriateness for sensing applications. The intelligent application of such nano-objects led to noticeably improved performances with increased sensitivities and lowered detection limits of several orders of magnitudes.

Some studies were conducted to determine MTX on nanomaterial fluorescent probes. Nanomaterial fluorescent sensors in comparison to the conventional fluorescence methodologies which

Table 4
The instrumental parameters for UV-visible spectrometry, capillary electrophoresis and electrochemical methods.

Sample	Preparation	Technique	Analyte	Instrumental parameters	Detector	LOD[a]	LOQ[a]	Linear range[a]	Recovery[a] (%)	Ref.
Pharmaceutical formulation and cell culture extract	-	EKC	D-MTX and L-MTX	A fused-silica capillary (120 cm × 75 μm) at room temperature conditioned with NaOH, H_2O, buffer, and BGE.	Phosphorescence detection	3.2×10^{-7} M	1.1×10^{-6} M	$r^2 \geq 0.9899$	-	[115]
CSF	SPE	CE	MTX and its metabolites	A fused-silica capillary (50.2 cm × 50 μm) conditioned with MeOH, H_2O, HCl 1 M, H_2O, NaOH 1 M, and H_2O.	UV at 300 nm	0.1 μM	0.5 μM	$r^2 \geq 0.9981$	22.4	[116]
Whole blood	SPE	CE	MTX and its metabolites	A fused-silica capillary (50.2 cm × 50 μm) at 25 °C conditioned with MeOH, H_2O, HCl 1 M, H_2O, NaOH 1 M, and H_2O.	UV at 300 nm	0.1 μM	NR	$r^2 \geq 0.9914$	-	[117]
Pharmaceutical formulation	-	MEKC	-	A fused-silica capillary (64.5 cm × 50 μm) at 25 °C conditioned with MeOH, NaOH 0.1 M, H_2O, MeOH, 0.1 M HCl, H_2O, and BGE.	UV at 254 nm	-	-	-	100-100.7	[118]
Bulk formulation	Dissolvation of drug in NaOH	UV-visible spectrophotometry	MTX	-	λ_1: 372[b], λ_2: 369-376 [c] nm	15.411[b], 14.0118 [c]	46.7 [b], 42.7067 [c]	3-15 μg/mL	98.54-99.36	[129]
Tablet	Dissolvation of drug in NaOH	UV-visible spectrophotometry	MTX	-	λ_1: 259[b], λ_2: 256-262 [c] nm	0.4779 [b], 9.3228 [c] μg/mL	28.401[b], 28.251[c] μg/mL	3-10 μg/mL	98.45-99.23	[130]
Bulk formulation	Dissolvation of drug with ASB	UV-visible spectrophotometry	MTX	-	λ_1: 258[b], λ_2: 250 [c], λ_3: 249-267 [d]nm	0.66 [b], 12.87 [c], 4.29 [d]	0.60 [b], 11.70 [c], 3.90 [d]	10-50 μg/mL	98.99-100.12	[131]
Tablet	Dissolvation of drug in NaOH	UV-visible spectrophotometry	MTX	-	λ_1: 258[b], λ_2: 252-264 [c] nm	108.04 [b], 11.51 [c]	360.15[b], 38.38 [c]	3-15 μg/mL	91.53-95.46	[132]
Bulk formulation	-	UV-visible spectrophotometry	MTX	-	λ_1: 303[b], λ_2: 294-308[c]nm	8.730 [b], 8.5011 [c]	28.57 [b], 28.3370 [c]	3-10 μg/mL	96.7-99.2	[133]
Urine	Mixed hemimicelles dispersive micro-solid phase extraction using ionic liquid functionalized magnetic graphene oxide/ polypyrrole	UV-visible spectrophotometry	MTX	-	UV at 375 nm	7 ng/mL	10 ng/mL	10-1000 ng/ mL	89-93	[134]
Tablet	Dissolvation of drug in NaOH	Electrochemical	MTX	m-AgSAE	CV, DPV and DCV	1.8 nM	-	2×10^{-9}-1×10^{-6} M	-	[135]
Tablet	Dissolvation of drug in H_2SO_4	Electrochemical	MTX	MWCNTs-DHP/GCE	DPAdSV	3.3×10^{-8} mol/ L	-	5.0×10^{-8}-5.0×10^{-6} mol/ L	2.62×10^{-9} mol cm^2	[138]
Urine	Dissolvation of drug in PBS	Electrochemical	MTX and CF	PABSA/Q-MWNTs/GCE	CV and DPV	0.015 μM	-	0.1-8.0 μM	94.0-107.3	[140]
Tablet and human blood serum	Removing of protein by ACN	Electrochemical	MTX	DNA/SWCNT/Nafion/GCE	SWASV	8.0×10^{-9} mol/ L		2.0×10^{-8}-1.5×10^{-6} mol/ L	96.5-110.0	[141]
Tablet	-	Electrochemical	MTX	$CoFe_2O_4$/IL-rGO/GCE	CV and DPV	0.01 nmol/mL	-	0.05-7.5 nmol/ mL	-	[142]
Tablet	Dissolvation of drug in NaOH	Electrochemical	MTX	PLL/GCE	FTIR, EIS and CV	1.7 nM	-	5 nM-0.2 μM	99.2-108.4	[143]
Pharmaceutical formulations	Dissolvation of drug in PBS	Electrochemical	MTX	BiFE	CV and DPAdSV	0.9 nM	-	12-1650 nM	-	[144]
Urine	-	Electrochemical	MTX	PdAg/NG-GCE	CV, EIS and DPV	1.32 nM	-	0.02-200 μM	-	[145]
Tablet and blood serum	Dissolvation of drug in PBS	Electrochemical	MTX	3DG-CNTN	CV and DPV	70 nM	-	7.0×10^{-7}-1.0×10^{-4} M	97.86-102.75	[146]
-	-	Electrochemical	MTX and DOX	CD-GNs/GCE	CV and DPV	20 nM	-	0.1-10 μM	-	[147]
PBS solution	Dissolvation of drug in PBS	Electrochemical	MTX	Antigen/Au electrode	EIS	1.65×10^{-10} M	-	2.76×10^{-4}-270×10^{-6} M	-	[148]
Urine		Electrochemical	MTX	dsDNA/GCE	CV and SWV	5.0×10^{-9}mol/L	-		99.40-104.0	[149]

	Dissolvation of drug in NaOH							2.0×10^{-8}- 4.0×10^{-6} mol/L		
Tablet and serum	Removing of protein by ACN	Electrochemical	MTX	Nano-Au/LC/GCE	CV and SWV	1.0×10^{-8} M	-	4.0×10^{-8}- 2×10^{-6}M	95.67-104.0	[150]
Tablet	Dissolvation of drug in NaOH	Electrochemical	MTX	p-AgSAE	CV, LSV and DPV	1.5×10^{-10} mol/L	-	5×10^{-10}- 3×10^{-6} M	97.4-104.0	[151]
Plasma and tablet	Dissolvatin of drug in deionized water	Electrochemical	MTX and ACV	EPPEG	CV and AdSWV	1.13×10^{-8} M	-	2×10^{-7}- 1.4×10^{-6} M	97.8-101.4	[152]
Urine and tablet	Dissolvation of drug in NaOH	Electrochemical	MTX	BDDE	CV, DPV and DCV	1.0×10^{-8} mol/L	-	5×10^{-8}- 2×10^{-5} M	99.2-101.4	[153]

CSF: cerebrospinal fluid, SPE: solid phase extraction, OrthoPhA: Orthophosphoric acid, ASB: anhydrous sodium carbonate, EKC: Electrokinetic chromatography, BGE: background electrolyte, CoFe2O4/IL-rGO/GCE: CoFe2O4 /ionic liquid/reduced graphene oxide/glassy carbon electrode, DPV: differential pulse voltammetry, PLL/GCE: poly (L-lysine)/ glassy carbon electrode, CV: cyclic voltammetry, FTIR: Fourier transform infrared spectroscopy, EIS: electrochemical impedance spectroscopy, MIP-SPE: molecularly imprinted solid-phase extraction, nano-Au/MWNTs-ZnO SPE: nano-Au/multi-walled carbon nanotubes-ZnO screen printed electrode, SWV: square wave voltammetry, PBS: phosphate buffer solution, CF: calcium folinate, PABSA/Q-MWNTs/GCE: p-aminobenzene sulfonic acid/quaternary amine functionalized multi-wall carbon nanotubes/glassy carbon electrode, EPI: epirubicin, dsDNA/GCE: double stranded DNA/glassy carbon electrode, LC: L-cysteine, BiFE: bismuth film modified electrode, DPAdSV: differential pulse adsorptive stripping voltammetry, ACN: acetonitrile, PdAg/NG-GCE: palladium-silver/N-graphene-glassy carbon electrode, LSV: linear sweep voltammetry, AgSAE: silver solid amalgam electrode, ACV: acyclovir, EPPEG: electropretreated pencil graphite electrode, AdSWV: adsorptive square wave voltammetry, DPAdSV: differential pulse adsorptive stripping voltammetry, MWCNTs-DHP/GCE: multiwalled functionalized carbon nanotubes-dihexadecylhydrogenphosphate/glassy carbon electrode, DNA/SWCNT: DNA/ single-walled carbon nanotube, SWASV: square wave anodic stripping voltammetry, 3DG-CNTN: 3D graphene-CNT network, CD-GNs/GCE: cyclodextrin-graphene hybrid nanosheets/glassy carbon electrode, DOX: doxorubicin, m-AgSAE: mercury silver solid amalgam electrode, DCV: direct current voltammetry, BDDE: Boron-doped diamond electrode, MEKC: micellar electrokinetic chromatography.

[a] Only for MTX.
[b] Method A.
[c] Method B.
[d] Method C.

need sophisticated derivatization to convert MTX into fluorescent compounds can offer a simple, easily operable and free of pretreatment processes method to determine MTX. These probes operate in accordance with the principles of fluorescence resonance energy transfer (FRET), inner filter effect (IFE), or electron transfer. Chen et al. introduced bovine serum albumin stabilized gold nanoclusters as fluorescence probes that yielded satisfactory results for MTX detection in real samples. The decrease in fluorescence intensity of the gold nanoclusters caused by MTX led to the sensitive determination of MTX in the range of 0.0016–24 μg/mL. The detection limit for MTX was reported to be 0.9 ng/mL [154]. Wang et al. synthesized N, S-codoped fluorescent carbon nanodots (NSCDs) by ammonium persulfate, glucose, and ethylene diamine that exhibited bright blue emission with a relatively high fluorescent quantum yield of 21.6%, good water solubility, uniform morphology, and excellent chemical stability, compared to pure CDs. The fluorescence of NSCDs significantly quenched by MTX via FRET between NSCDs and MTX, which was used for highly selective and sensitive detection of MTX with a wide linear range up to 50.0 μM and a low detection limit of 0.33 nM. The method was applied successfully for the detection of MTX in human serum [155]. Recently, Zhao et al. prepared N, S co-doped carbon quantum dots, using citric acid and L-cysteine which could be easily quenched by MTX on the basis of IFE. The probe displayed high sensitivity and specific selectivity with a linear detection range of 0.4–41.3 μg/mL and a low detection limit of 12 ng/mL [156]. Simultaneous detection of FA and MTX by an optical sensor based on MIPs on dual-color CdTe quantum dots was reported by Ensafi et al. The dynamic range was 0.5–20 μM, and the detection limits for FA and MTX were 32.0 and 34.0 nM, respectively. The method was successfully applied for the simultaneous detection of FA and MTX in human blood plasma samples [157].

12. Conclusion

This review investigated the analysis of MTX and its metabolites from 2008 up to 2019. Literature review revealed that different analytical techniques such as HPLC using different detector systems, UV–visible spectrophotometry, electrochemical methods and capillary electrophoresis have been employed to determine MTX and its metabolites in pharmaceutical, biological, and environmental samples. Comparison of these analytical methodologies is shown in Fig. 2. As demonstrated, LC-MS, with good selectivity and low LOQ, is the most frequently used technique for MTX analysis in biological and environmental samples. HPLC was found to be an accurate method for MTX measurement. Due to polarity of the molecules and the relatively low water solubility, the reported methods for the assay of this drug are mostly reversed-phase HPLC methods using C_{18} silica stationary phases and mixtures of polar solvents as mobile phases. New HPLC methods using stationary phases with different retention mechanisms have been presented. HPLC equipped with fluorescence detector is more selective and sensitive than UV–visible detector, but MTX and its metabolites are not fluorescent. Therefore, oxidative degradation is used to produce fluorescence products. Electrochemical techniques, with low LOD, as a simple, selective, and sensitive method, have been used to measure MTX in pharmaceutical and biological samples. Numerous electrodes have been modified with different nanomaterials such as multiwall carbon nanotubes, silver- and magnetic nanoparticles to increase the efficacy of electrochemical identification. UV–visible spectrophotometry has been only used to determine MTX in pharmaceutical samples. Several methods including the enzyme-multiplied immunoassay technique (EMIT), enzyme inhibition assays, the fluorescence polarization immunoassay (FPIA) as well as HPLC methods coupled with UV, fluorescence or mass

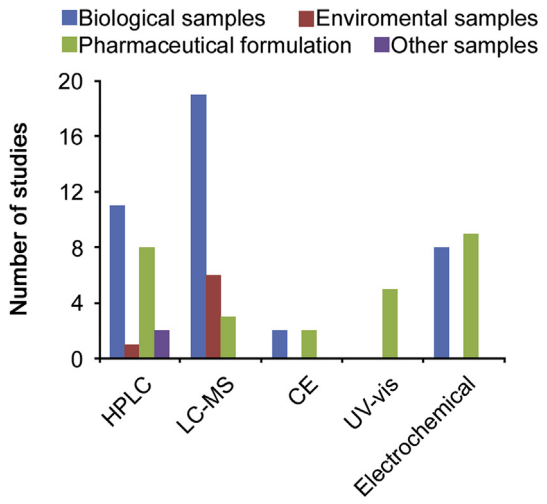

Fig. 2. Comparison of instrumental techniques and various samples reported for MTX and its metabolites determination.

spectrometer detectors have been developed for routine monitoring of MTX concentrations in biological samples. However, the instrumentation and reagents are costly, hence not available in all clinical laboratories. Furthermore, HPLC is time-consuming and labor intensive, and thus it is less commonly employed in clinical settings. Due to such analytical limitations, alternative methodologies to analyze MTX are warranted. Research on nanomaterial optical sensors-based methods might lead us to a new horizon to overcome the limitations and develop alternative approaches.

Acknowledgments

The authors wish to thank the support of the Vice-Chancellor for Research, Shiraz University of Medical Sciences, Iran (project No. 97-01-36-18308). The authors also wish to thank Mr. H. Argasi at the Research Consultation Center (RCC) of Shiraz University of Medical Sciences for his invaluable assistance in editing this manuscript.

Conflicts of interest

The authors declare that there are no conflicts of interest.

References

[1] M. Visentin, R. Zhao, I.D. Goldman, The antifolates, Hematol. Oncol. Clin. N. Am. 26 (2012) 629–648.
[2] W.M. Hryniuk, J.R. Bertino, Treatment of leukemia with large doses of methotrexate and folinic acid: clinical-biochemical correlates, J. Clin. Investig. 48 (1969) 2140–2155.
[3] J.R. Bertino, M.B. Mosher, R.C. Deconti, Chemotherapy of cancer of the head and neck, Cancer 31 (1973) 1141–1149.
[4] A.K. Sinha, S. Anand, B.J. Ortel, et al., Methotrexate used in combination with aminolaevulinic acid for photodynamic killing of prostate cancer cells, Br. J. Canc. 95 (2006) 485.
[5] R.B. Natale, A. Yagoda, R.C. Watson, et al., Methotrexate: an active drug in bladder cancer, Cancer 47 (1981) 1246–1250.
[6] P. Cipriani, P. Ruscitti, F. Carubbi, et al., Methotrexate: an old new drug in autoimmune disease, Expert Rev. Clin. Immunol. 10 (2014) 1519–1530.
[7] B. Ramachandra, Development of impurity profiling methods using modern analytical techniques, Crit. Rev. Anal. Chem. 47 (2017) 24–36.
[8] A.F. Hawwa, A. AlBawab, M. Rooney, et al., Methotrexate polyglutamates as a potential marker of adherence to long-term therapy in children with juvenile idiopathic arthritis and juvenile dermatomyositis: an observational, cross-sectional study, Arthritis Res. Ther. 17 (2015) 295.
[9] P. Rajnics, V.S. Kellner, A. Kellner, et al., The hematologic toxicity of methotrexate in patients with autoimmune disorders, J. Neoplasm. 2 (2017) 1–6.
[10] A. Weidmann, A.C. Foulkes, N. Kirkham, et al., Methotrexate toxicity during treatment of chronic plaque psoriasis: a case report and review of the literature, Dermatol. Ther. 4 (2014) 145–156.
[11] T. Gabbani, S. Deiana, S. Lunardi, et al., Safety profile of methotrexate in inflammatory bowel disease, Expert Opin. Drug Saf. 15 (2016) 1427–1437.
[12] S.C. Howard, J. McCormick, C.H. Pui, et al., Preventing and managing toxicities of high-dose methotrexate, Oncol. 21 (2016) 1471–1482.
[13] B.C. Widemann, P.C. Adamson, Understanding and managing methotrexate nephrotoxicity, Oncol. 11 (2006) 694–703.
[14] A.P. Garneau, J. Riopel, P. Isenring, Acute methotrexate-induced crystal nephropathy, N. Engl. J. Med. 373 (2015) 2691–2693.
[15] A. Garcia-Ac, P.A. Segura, L. Viglino, et al., Comparison of APPI, APCI and ESI for the LC-MS/MS analysis of bezafibrate, cyclophosphamide, enalapril, methotrexate and orlistat in municipal wastewater, J. Mass Spectrom. 46 (2011) 383–390.
[16] S. Nussbaumer, L. Geiser, F. Sadeghipour, et al., Wipe sampling procedure coupled to LC-MS/MS analysis for the simultaneous determination of 10 cytotoxic drugs on different surfaces, Anal. Bioanal. Chem. 402 (2012) 2499–2509.
[17] N. Guichard, D. Guillarme, P. Bonnabry, et al., Antineoplastic drugs and their analysis: a state of the art review, Analyst 142 (2017) 2273–2321.
[18] E.S. Chan, B.N. Cronstein, Methotrexate-how does it really work? Nat. Rev. Rheumatol. 6 (2010) 175–178.
[19] J.C. White, I.D. Goldman, Mechanism of action of methotrexate, Mol. Pharmacol. 12 (1976) 711–719.
[20] D. Levêque, G. Becker, E. Toussaint, et al., Clinical pharmacokinetics of methotrexate in oncology, Int. J. Pharmacokinet. 2 (2017) 137–147.
[21] D.D. Shen, D.L. Azarnoff, Clinical pharmacokinetics of methotrexate, Clin. Pharmacokinet. 3 (1978) 1–13.
[22] D.A. Cairnes, W.E. Evans, A simple preparation of the methotrexate metabolites 7-hydroxymethotrexate and 4-deoxy-4-amino-N10-methylpteroic acid, Ther. Drug Monit. 5 (1983) 363–366.
[23] B.A. Chabner, C.J. Allegra, G.A. Curt, et al., Polyglutamation of methotrexate. Is methotrexate a prodrug? J. Clin. Investig. 76 (1985) 907–912.
[24] T. Dervieux, T.L. Brenner, Y.Y. Hon, et al., De novo purine synthesis inhibition and antileukemic effects of mercaptopurine alone or in combination with methotrexate in vivo, Blood 100 (2002) 1240–1247.
[25] P. Angelis-Stoforidis, F.J.E. Vajda, N. Christophidis, Methotrexate polyglutamate levels in circulating erythrocytes and polymorphs correlate with clinical efficacy in rheumatoid arthritis, Clin. Exp. Rheumatol. 17 (1999) 313–320.
[26] J. Chládek, J. Martínková, M. Simková, et al., Pharmacokinetics of low doses of methotrexate in patients with psoriasis over the early period of treatment, Eur. J. Clin. Pharmacol. 53 (1998) 437–444.
[27] K. Schmiegelow, H. Schrøder, G. Gustafsson, et al., Risk of relapse in childhood acute lymphoblastic leukemia is related to RBC methotrexate and mercaptopurine metabolites during maintenance chemotherapy. Nordic Society for Pediatric Hematology and Oncology, J. Clin. Oncol. 13 (1995) 345–351.
[28] T. Dervieux, D. Furst, D.O. Lein, et al., Polyglutamation of methotrexate with common polymorphisms in reduced folate carrier, aminoimidazole carboxamide ribonucleotide transformylase, and thymidylate synthase are associated with methotrexate effects in rheumatoid arthritis, Arthritis Rheum. 50 (2004) 2766–2774.
[29] T. Dervieux, J. Kremer, D.O. Lein, et al., Contribution of common polymorphisms in reduced folate carrier and γ-glutamylhydrolase to methotrexate polyglutamate levels in patients with rheumatoid arthritis, Pharmacogenetics Genom. 14 (2004) 733–739.
[30] W.A. Bleyer, The clinical pharmacology of methotrexate: New applications of an old drug, Cancer 41 (1978) 36–51.
[31] S.N. Reiss, L.W. Buie, N. Adel, et al., Hypoalbuminemia is significantly associated with increased clearance time of high dose methotrexate in patients being treated for lymphoma or leukemia, Ann. Hematol. 95 (2016) 2009–2015.
[32] J. Li, P. Gwilt, The effect of malignant effusions on methotrexate disposition, Cancer Chemother. Pharmacol. 50 (2002) 373–382.
[33] W.A. Bleyer, Methotrexate: clinical pharmacology, current status and therapeutic guidelines, Cancer Treat Rev. 4 (1977) 87–101.
[34] E. Raude, M. Oellerich, M. Wrenger, Methotrexate: specific HPLC routine method involving column switching, Fresenius Z. Anal. Chem. 330 (1988) 384–385.
[35] F. Palmisano, A. Guerrieri, P.G. Zambonin, et al., Determination of methotrexate in untreated body fluids by micellar liquid chromatography, Anal. Chem. 61 (1989) 946–950.
[36] C. Sottani, R. Turci, L. Perbellini, et al., Liquid–liquid extraction procedure for trace determination of cyclophosphamide in human urine by high-performance liquid chromatography tandem mass spectrometry, Rapid Commun. Mass Spectrom. 12 (1998) 1063–1068.
[37] M. Uchiyama, T. Matsumoto, T. Matsumoto, et al., Simple and sensitive HPLC method for the fluorometric determination of methotrexate and its major metabolites in human plasma by post-column photochemical reaction, Biomed. Chromatogr. 26 (2012) 76–80.
[38] M. Montemurro, María M. De Zan, J.C. Robles, Optimized high performance liquid chromatography–ultraviolet detection method using core-shell particles for the therapeutic monitoring of methotrexate, J. Pharm. Anal. 6 (2016) 103–111.

[39] Y.-D. Li, Y. Li, N.-S. Liang, et al., A reversed-phase high performance liquid chromatography method for quantification of methotrexate in cancer patients serum, J. Chromatogr. B 1002 (2015) 107–112.
[40] X. Liu, J. Liu, Y. Huang, et al., Determination of methotrexate in human serum by high-performance liquid chromatography combined with pseudo template molecularly imprinted polymer, J. Chromatogr., A 1216 (2009) 7533–7538.
[41] L. van Haandel, M.L. Becker, J.S. Leeder, et al., A novel high-performance liquid chromatography/mass spectrometry method for improved selective and sensitive measurement of methotrexate polyglutamation status in human red blood cells, Rapid Commun. Mass Spectrom. 23 (2009) 3693–3702.
[42] R.J.W. Meesters, E. den Boer, R. de Jonge, et al., Assessment of intracellular methotrexate and methotrexatepolyglutamate metabolite concentrations in erythrocytes by ultrafast matrix-assisted laser desorption/ionization triple quadrupole tandem mass spectrometry, Rapid Commun. Mass Spectrom. 25 (2011) 3063–3070.
[43] A.F. Hawwa, A. AlBawab, M. Rooney, et al., A novel dried blood spot-LCMS method for the quantification of methotrexate polyglutamates as a potential marker for methotrexate use in children, PLoS One 9 (2014), e89908.
[44] N. Masque, R. Marcé, F. Borrull, New polymeric and other types of sorbents for solid-phase extraction of polar organic micropollutants from environmental water, Trends Anal. Chem. 17 (1998) 384–394.
[45] L. Nováková, H. Vlčková, A review of current trends and advances in modern bio-analytical methods: chromatography and sample preparation, Anal. Chim. Acta 656 (2009) 8–35.
[46] S. Sigma-Aldrich, Guide to solid phase extraction-bulletin 910, Bull. (Arch. Am. Art) 910 (1998).
[47] M.A. Al-Ghobashy, S.A. Hassan, D.H. Abdelaziz, et al., Development and validation of LC-MS/MS assay for the simultaneous determination of methotrexate, 6-mercaptopurine and its active metabolite 6-thioguanine in plasma of children with acute lymphoblastic leukemia: correlation with genetic polymorphism, J. Chromatogr B. Analyt. Technol. Biomed. Life Sci. 1038 (2016) 88–94.
[48] P.I. Mathias, T.H. Connor, C. B'Hymer, A review of high performance liquid chromatographic-mass spectrometric urinary methods for anticancer drug exposure of health care workers, J. Chromatogr. B 1060 (2017) 316–324.
[49] R. Turci, M.L. Fiorentino, C. Sottani, et al., Determination of methotrexate in human urine at trace levels by solid phase extraction and high-performance liquid chromatography/tandem mass spectrometry, Rapid Commun. Mass Spectrom. 14 (2000) 173–179.
[50] B. Petrie, J. Youdan, R. Barden, et al., Multi-residue analysis of 90 emerging contaminants in liquid and solid environmental matrices by ultra-high-performance liquid chromatography tandem mass spectrometry, J. Chromatogr. A 1431 (2016) 64–78.
[51] V. Flotron, J. Houessou, A. Bosio, et al., Rapid determination of polycyclic aromatic hydrocarbons in sewage sludges using microwave-assisted solvent extraction: comparison with other extraction methods, J. Chromatogr. A 999 (2003) 175–184.
[52] M. Hroch, J. Tuková, P. Doležalová, et al., An improved high-performance liquid chromatography method for quantification of methotrexate polyglutamates in red blood cells of children with juvenile idiopathic arthritis, Biopharm Drug Dispos. 30 (2009) 138–148.
[53] W.R. Alahmad, M.A. Alawi, Hplc/Uv/fluorescence detection of several pharmaceuticals in sewage treatment plant wastewaters of Jordan, Fresenius Environ. Bull. 19 (2010) 805–810.
[54] Z. Zhu, H. Wu, S. Wu, et al., Determination of methotrexate and folic acid by ion chromatography with electrochemical detection on a functionalized multi-wall carbon nanotube modified electrode, J. Chromatogr. A 1283 (2013) 62–67.
[55] A. Jones, S. Pravadali-Cekic, G.R. Dennis, et al., Post column derivatisation analyses review. Is post-column derivatisation incompatible with modern HPLC columns? Anal. Chim. Acta 889 (2015) 58–70.
[56] J. Ciekot, T. Goszczyński, J. Boratyński, Methods for methotrexate determination in macromolecular conjugates drug carrier, Acta Pol. Pharm. 69 (2012) 1342–1346.
[57] S. Fekete, A. Beck, J.-L. Veuthey, et al., Theory and practice of size exclusion chromatography for the analysis of protein aggregates, J. Pharm. Biomed. Anal. 101 (2014) 161–173.
[58] K. Michaila, M.S. Moneeb, Determination of methotrexate and indomethacin in urine using SPE-LC-DAD after derivatization, J. Pharm. Biomed. Anal. 55 (2011) 317–324.
[59] E. Begas, C. Papandreou, A. Tsakalof, et al., Simple and reliable HPLC method for the monitoring of methotrexate in osteosarcoma patients, J. Chromatogr. Sci. 52 (2014) 590–595.
[60] L. Hu, Y. Liu, S. Cheng, Simultaneous determination of six analytes by HPLC-UV for high throughput analysis in permeability assessment, J. Chromatogr. Sci. 49 (2011) 124–128.
[61] T. Hirai, S. Matsumoto, I. Kishi, Simultaneous analysis of several non-steroidal anti-inflammatory drugs in human urine by high-performance liquid chromatography with normal solid-phase extraction, J. Chromatogr. B Biomed. Sci. Applic. 692 (1997) 375–388.
[62] L. Nováková, L. Matysová, L. Havlíková, et al., Development and validation of HPLC method for determination of indomethacin and its two degradation products in topical gel, J. Pharm. Biomed. Anal. 37 (2005) 899–905.
[63] S. Hess, U. Teubert, J. Ortwein, et al., Profiling indomethacin impurities using high-performance liquid chromatography and nuclear magnetic resonance, Eur. J. Pharm. Sci. 14 (2001) 301–311.
[64] M.S. Iqbal, M.A. Shad, M.W. Ashraf, et al., Development and Validation of an HPLC Method for the determination of Dexamethasone, Dexamethasone sodium phosphate and chloramphenicol in presence of each other in pharmaceutical preparations, Chromatographia 3 (2006) 219–222.
[65] Y.-K. Song, J.-S. Park, J.-K. Kim, et al., HPLC determination of dexamethasone in human plasma, J. Liq. Chromatogr. Relat. Technol. 27 (2004) 2293–2306.
[66] Ł. Skibińska, J. Gregorczyk, A. Jarmołowicz, HPLC determination of methotrexate and its metabolites in blood plasma, Chem. Anal. 50 (2005) 551–560.
[67] H. Li, W. Luo, Q. Zeng, et al., Method for the determination of blood methotrexate by high performance liquid chromatography with online post-column electrochemical oxidation and fluorescence detection, J. Chromatogr. B Analyt. Technol. Biomed. Life Sci. 845 (2007) 164–168.
[68] N.K. Lariya, G.P. Agrawal, Development and validation of RP-HPLC method for simultaneous determination of methotrexate, dexamethasone and indomethacin, Int. J. Pharm. Pharm. Sci. 7 (2014) 443–446.
[69] A. Agrawal, M. Sharma, RP-HPLC estimation of methotrexate and tretinoin in bulk and pharmaceutical dosage forms, J. Drug Discov. Ther. 5 (2017) 9–20.
[70] C.-S. Wu, C.-H. Wang, J.-L. Zhang, et al., Separation, determination of six impurities in methotrexate drug substance using ultra-performance liquid chromatography, Chin. Chem. Lett. 25 (2014) 447–450.
[71] H. Fessi, F. Puisieux, J.P. Devissaguet, et al., Nanocapsule formation by interfacial deposition following solvent displacement, Int. J. Pharm. 55 (1989) R1–R4.
[72] J. M Barichello, M. Morishita, K. Takayama, et al., Encapsulation of hydrophilic and lipophilic drugs in PLGA nanoparticles by the nanoprecipitation method, Drug Dev. Ind. Pharm. 25 (1999) 471–476.
[73] S. Galindo-Rodriguez, E. Allemann, H. Fessi, et al., Physicochemical parameters associated with nanoparticle formation in the salting-out, emulsification-diffusion, and nanoprecipitation methods, Pharm. Res. (N. Y.) 21 (2004) 1428–1439.
[74] F. Ganachaud, J.L. Katz, Nanoparticles and nanocapsules created using the ouzo effect: spontaneous emulsification as an alternative to ultrasonic and high-shear devices, ChemPhysChem 6 (2005) 209–216.
[75] B.V.N. Nagavarma, H.K.S. Yadav, A. Ayaz, et al., Different techniques for preparation of polymeric nanoparticles-a review, Asian J. Pharmaceut. Clin. Res. 5 (2012) 16–23.
[76] T. Niwa, H. Takeuchi, T. Hino, et al., Preparation of biodegradable nanoparticles of water-soluble and insoluble drugs with D, L lactide/glycolide copolymer by a novel spontaneous emulsification solvent diffusion method, and the drug release behavior, J. Control. Release 25 (1993) 89–98.
[77] N.K. Garg, G. Sharma, B. Singh, et al., Quality by design (QbD)-based development and optimization of a simple, robust RP-HPLC method for the estimation of methotrexate, J. Liq. Chromatogr. Relat. Technol. 38 (2015) 1629–1637.
[78] A. Azadi, M.-R. Rouini, M. Hamidi, Neuropharmacokinetic evaluation of methotrexate-loaded chitosan nanogels, Int. J. Biol. Macromol. 79 (2015) 326–335.
[79] V.J. Mohanraj, Y. Chen, Nanoparticles a review, Int. J. Pharm. Pharmaceut. Res. 5 (2006) 561–573.
[80] A.R. Oliveira, L.B. Caland, E.G. Oliveira, et al., HPLC-DAD and UV-Vis spectrophotometric methods for methotrexate assay in different biodegradable microparticles, J. Braz. Chem. Soc. 26 (2015) 649–659.
[81] V. Raichur, V.K. Devi, Development and validation of a highly sensitive high-performance liquid chromatography (HPLC) method for the estimation of methotrexate (MTX) pure drug and marketed formulation in spiked rat plasma, Int. J. Pharm. Pharmaceut. Res. 8 (2016) 313–317.
[82] M. Roy, M. Mohite, S. Shah, Development and validation of RP-HPLC method for the determination of methotrexate in bulk and pharmaceutical tablet dosage form, Eur. J. Pharm. Med. Res. 3 (2016) 355–358.
[83] F. Ullah, Z. Iqbal, A. Raza, et al., Simultaneous determination of methotrexate and metoclopramide in physiological fluids using RP-HPLC with ultra-violet detection; application in evaluation of polymeric nanoparticles, J. Liq. Chromatogr. Relat. Technol. 40 (2017) 1020–1030.
[84] T. Sartori, F.S. Murakami, A.P. Cruz, et al., Development and validation of a fast RP-HPLC method for determination of methotrexate entrapment efficiency in polymeric nanocapsules, J. Chromatogr. Sci. 46 (2008) 505–509.
[85] S. Fang, C.P. Lollo, C. Derunes, et al., Development and validation of a liquid chromatography method for simultaneous determination of three process-related impurities: yeastolates, triton X-100 and methotrexate, J. Chromatogr. B 879 (2011) 3612–3619.
[86] E. de Hoffmann, Tandem mass spectrometry: a primer, J. Mass Spectrom. 31 (1996) 129–137.
[87] M. Petrović, M.D. Hernando, M.S. Díaz-Cruz, et al., Liquid chromatography-tandem mass spectrometry for the analysis of pharmaceutical residues in environmental samples: a review, J. Chromatogr. A 1067 (2005) 1–14.
[88] S. Thappali, K. Varanasi, S. Veeraraghavan, et al., Simultaneous determination of methotrexate, dasatinib and its active metabolite N-deshydroxyethyl dasatinib in rat plasma by LC-MS/MS: method validation and application to pharmacokinetic study, Arzneimittelforschung 62 (2012) 624–630.
[89] I. Rodin, A. Braun, A. Stavrianidi, et al., A validated LC–MS/MS method for rapid determination of methotrexate in human saliva and its application toan excretion evaluation study, J. Chromatogr. B 937 (2013) 1–6.
[90] C.-S. Wu, Y.-F. Tong, P.-Y. Wang, et al., Identification of impurities in

methotrexate drug substances using high-performance liquid chromatography coupled with a photodiode array detector and Fourier transform ion cyclotron resonance mass spectrometry, Rapid Commun. Mass Spectrom. 27 (2013) 971–978.
[91] T. Dervieux, D.O. Lein, J. Marcelletti, et al., HPLC determination of erythrocyte methotrexate polyglutamates after low-dose methotrexate therapy in patients with rheumatoid arthritis, Clin. Chem. 49 (2003) 1632–1641.
[92] S. Nussbaumer, S. Fleury-Souverain, P. Antinori, et al., Simultaneous quantification of ten cytotoxic drugs by a validated LC–ESI–MS/MS method, Anal. Bioanal. Chem. 398 (2010) 3033–3042.
[93] M. Jeronimo, M. Colombo, G. Astrakianakis, et al., A surface wipe sampling and LC–MS/MS method for the simultaneous detection of six antineoplastic drugs commonly handled by healthcare workers, Anal. Bioanal. Chem. 407 (2015) 7083–7092.
[94] X. Mo, Y. Wen, B. Ren, et al., Determination of erythrocyte methotrexate polyglutamates by liquid chromatography/tandem mass spectrometry after low-dose methotrexate therapy in Chinese patients with rheumatoid arthritis, J. Chromatogr. B Analyt. Technol. Biomed. Life Sci. 907 (2012) 41–48.
[95] G. Chen, J.P. Fawcett, M. Mikov, et al., Simultaneous determination of methotrexate and its polyglutamate metabolites in Caco-2 cells by liquid chromatography-tandem mass spectrometry, J. Pharm. Biomed. Anal. 50 (2009) 262–266.
[96] E. Sonemoto, N. Kono, R. Ikeda, et al., Practical determination of methotrexate in serum of rheumatic patients by LC/MS/MS, Biomed. Chromatogr. 26 (2012) 1297–1300.
[97] V. Upadhyay, Mansingh Rajput, A. Sen, et al., A sensitive, high throughput estimation of methotrexate in human plasma by high performance liquid chromatography tandem mass spectrometry, Int. J. Pharm. Sci. Res. 8 (2017) 3371–3378.
[98] M.B. Mulder, R. Huisman, F.K. Engels, et al., Therapeutic Drug Monitoring of methotrexate in plasma using U-HPLC-MS/MS: necessary after administration of glucarpidase in methotrexate intoxications, Ther. Drug Monit. 40 (2018) 383–385, https://doi.org/10.1097/FTD.0000000000000515.
[99] D. Wu, Y. Wang, Y. Sun, et al., A simple, rapid and reliable liquid chromatography-mass spectrometry method for determination of methotrexate in human plasma and its application to therapeutic drug monitoring, Biomed. Chromatogr. 29 (2015) 1197–1202.
[100] E. den Boer, S.G. Heil, B.D. van Zelst, et al., A U-HPLC-ESI-MS/MS-based stable isotope dilution method for the detection and quantitation of methotrexate in plasma, Ther. Drug Monit. 34 (2012) 432–439.
[101] S. Mei, X. Shi, Y. Du, et al., Simultaneous determination of plasma methotrexate and 7-hydroxy methotrexate by UHPLC-MS/MS in patients receiving high-dose methotrexate therapy, J. Pharm. Biomed. Anal. 158 (2018) 300–306.
[102] N. Guichard, S. Fekete, D. Guillarme, et al., Computer-assisted UHPLC–MS method development and optimization for the determination of 24 antineoplastic drugs used in hospital pharmacy, J. Pharm. Biomed. Anal. 164 (2019) 395–401.
[103] E. den Boer, R.J. Meesters, B.D. Van Zelst, et al., Measuring methotrexate polyglutamates in red blood cells: a new LC-MS/MS-based method, Anal. Bioanal. Chem. 405 (2013) 1673–1681.
[104] V. Ganti, E.A. Walker, S. Nagar, Pharmacokinetic application of a bioanalytical LC-MS method developed for 5-fluorouracil and methotrexate in mouse plasma, brain and urine, Biomed. Chromatogr. 27 (2013) 994–1002.
[105] K. Sharma, K. Giri, V. Dhiman, et al., A validated LC-MS/MS assay for simultaneous quantification of methotrexate and tofacitinib in rat plasma: application to a pharmacokinetic study, Biomed. Chromatogr. 29 (2015) 722–732.
[106] R.C. Schofield, L.V. Ramanathan, K. Murata, et al., Development and validation of a turbulent flow chromatography and tandem mass spectrometry method for the quantitation of methotrexate and its metabolites 7-hydroxy methotrexate and DAMPA in serum, J. Chromatogr B Analyt. Technol. Biomed. Life Sci. 1002 (2015) 169–175.
[107] A.M. Stolker, R.J.B. Peters, R. Zuiderent, et al., Fully automated screening of veterinary drugs in milk by turbulent flow chromatography and tandem mass spectrometry, Anal. Bioanal. Chem. Rev. 397 (2010) 2841–2849.
[108] A. Garcia-Ac, P.A. Segura, C. Gagnon, et al., Determination of bezafibrate, methotrexate, cyclophosphamide, orlistat and enalapril in waste and surface waters using on-line solid-phase extraction liquid chromatography coupled to polarity-switching electrospray tandem mass spectrometry, J. Environ. Monit. 11 (2009) 830–838.
[109] M. Canal-Raffin, K. Khennoufa, B. Martinez, et al., Highly sensitive LC-MS/MS methods for urinary biological monitoring of occupational exposure to cyclophosphamide, ifosfamide, and methotrexate antineoplastic drugs and routine application, J. Chromatogr. B 1038 (2016) 109–117.
[110] F. Dal Bello, V. Santoro, V. Scarpino, et al., Antineoplastic drugs determination by HPLC-HRMSn to monitor occupational exposure, Drug Test. Anal. 8 (2016) 730–737.
[111] J. Bluett, I. Riba-Garcia, K. Hollywood, et al., A HPLC-SRM-MS based method for the detection and quantification of methotrexate in urine at doses used in clinical practice for patients with rheumatological disease: a potential measure of adherence, Analyst 140 (2015) 1981–1987.
[112] N. Anastos, N.W. Barnett, S.W. Lewis, Capillary electrophoresis for forensic drug analysis: a review, Talanta 67 (2005) 269–279.
[113] G. Hempel, Strategies to improve the sensitivity in capillary electrophoresis for the analysis of drugs in biological fluids, Electrophoresis 21 (2000) 691–698.
[114] D.K. Lloyd, Capillary electrophoretic analyses of drugs in body fluids: sample pretreatment and methods for direct injection of biofluids, J. Chromatogr., A 735 (1996) 29–42.
[115] M. Castro-Puyana, I. Lammers, J. Buijs, et al., Quenched phosphorescence as alternative detection mode in the chiral separation of methotrexate by electrokinetic chromatography, Anal. Bioanal. Chem. 400 (2011) 2913–2919.
[116] H.L. Cheng, S.S. Chiou, Y.M. Liao, et al., Analysis of methotrexate and its eight metabolites in cerebrospinal fluid by solid-phase extraction and triple-stacking capillary electrophoresis, Anal. Bioanal. Chem. 398 (2010) 2183–2190.
[117] H.L. Cheng, Y.M. Liao, S.S. Chiou, et al., On-line stacking capillary electrophoresis for analysis of methotrexate and its eight metabolites in whole blood, Electrophoresis 29 (2008) 3665–3673.
[118] N. Guichard, M. Ogereau, L. Falaschi, et al., Determination of 16 antineoplastic drugs by capillary electrophoresis with UV detection: applications in quality control, Electrophoresis 39 (2018) 2512–2520.
[119] R.-I. Stefan, R.G. Bokretsion, J.F. van Staden, et al., Simultaneous determination of creatine and creatinine using amperometric biosensors, Talanta 60 (2003) 1223–1228.
[120] D.A. El-Hady, M.M. Seliem, R. Gotti, et al., Novel voltammetric method for enantioseparation of racemic methotrexate: determination of its enantiomeric purity in some pharmaceuticals, Sens. Actuators B Chem. 113 (2006) 978–988.
[121] A.A. Rat'ko, R.I. Stefan, J.F. van Staden, et al., Macrocyclic antibiotics as chiral selectors in the design of enantioselective, potentiometric membrane electrodes for the determination of L- and D-enantiomers of methotrexate, Talanta 64 (2004) 145–150.
[122] J. Subert, K. Slais, Progress in the separation of enantiomers of chiral drugs by TLC without their prior derivatization, Pharmazie 56 (2001) 355–360.
[123] S.M. Cramer, J.H. Schornagel, K.K. Kalghatgi, et al., Occurrence and significance of d-methotrexate as a contaminant of commercial methotrexate, Cancer Res. 44 (1984) 1843–1846.
[124] D.W. Armstrong, K.L. Rundlett, J.-R. Chen, Evaluation of the macrocyclic antibiotic vancomycin as a chiral selector for capillary electrophoresis, Chirality 6 (1994) 496–509.
[125] U.B. Nair, D.W. Armstrong, W.L. Hinze, Characterization and evaluation of d-(+)-tubocurarine chloride as a chiral selector for capillary electrophoretic enantioseparations, Anal. Chem. 70 (1998) 1059–1065.
[126] S. Lee, S. Jung, Enantioseparation using cyclosophoraoses as a novel chiral additive in capillary electrophoresis, Carbohydr. Res. 338 (2003) 1143–1146.
[127] F.M. Rubino, Separation methods for methotrexate, its structural analogues and metabolites, J. Chromatogr. B Biomed. Sci. Applic. 764 (2001) 217–254.
[128] C.B. Ojeda, F.S. Rojas, Recent developments in derivative ultraviolet/visible absorption spectrophotometry, Anal. Chim. Acta 518 (2004) 1–24.
[129] P. Shinde, S.J. Suryawanshi, P.B. Jadhav, et al., Spectrophotometric determination of methotrexate by zero order derivative and area under curve method, Int. J. Appl. Pharm. 2 (2015) 54–61.
[130] S.U. Gadve, P.P. Hulle, M.B. Shelke, et al., Development of uv- visible spectrophotometric method for the analysis of methotrexate in tablet formulations, Int. J. Pharm. Chem. Biol. Sci. 5 (2015) 982–985.
[131] M. Pratapwar, D. Sabane, A. Khilari, et al., To study the effect of anhydrous solvent on methotrexate by using uv-spectrophotometer, World J. Pharm. Pharmaceut. Sci. 6 (2017) 904–911.
[132] S. Suryawanshi, P. Shinde, N. Thamke, et al., Spectrophotometric determination of methotrexate in tablet dosage form, Eur. J. Pharm. Med. Res. 2 (2015) 153–155.
[133] P. Faijal, S. Maroti, S. Samrat, A UV-spectrophotometric determination of methotrexate in tablet dosage form, Int. J. Res. Pharm. Chem. 5 (2015) 641–644.
[134] S. Hamidi, A. Azami, E.M. Aghdam, A novel mixed hemimicelles dispersive micro-solid phase extraction using ionic liquid functionalized magnetic graphene oxide/polypyrrole for extraction and pre-concentration of methotrexate from urine samples followed by the spectrophotometric method, Clin. Chim. Acta 488 (2018) 179–188.
[135] R. Šelešovská, L. Bandžuchová, T. Navrátil, Voltammetric behavior of methotrexate using mercury meniscus modified silver solid amalgam electrode, Electroanalysis 23 (2011) 177–187.
[136] R.C. Gurira, L. Bowers, Electrochemistry of methotrexate: Part I. Characteristics of reduction, J. Electroanal. Chem. 146 (1983) 109–122.
[137] B.C. Janegitz, R. Pauliukaite, M.E. Ghica, et al., Direct electron transfer of glucose oxidase at glassy carbon electrode modified with functionalized carbon nanotubes within a dihexadecylphosphate film, Sensor. Actuator. B Chem. 158 (2011) 411–417.
[138] G.G. Oliveira, B.C. Janegitz, V. Zucolotto, et al., Differential pulse adsorptive stripping voltammetric determination of methotrexate using a functionalized carbon nanotubes-modified glassy carbon electrode, Cent. Eur. J. Chem. 11 (2013) 1837–1843.
[139] H.R.S. Lima, J.S. da Silva, E.A. de O. Farias, et al., Electrochemical sensors and biosensors for the analysis of antineoplastic drugs, Biosens. Bioelectron. 108 (2018) 27–37.
[140] Z. Zhu, F. Wang, F. Wang, et al., Simultaneous determination of methotrexate and calcium folinate with electrochemical method based on a poly-ABSA/

functionalized MWNTs composite film modified electrode, J. Electroanal. Chem. 708 (2013) 13–19.
[141] Y. Wang, H. Liu, F. Wang, et al., Electrochemical oxidation behavior of methotrexate at DNA/SWCNT/Nafion composite film-modified glassy carbon electrode, J. Solid State Electrochem. 16 (2012) 3227–3235.
[142] A.A. Ensafi, F. Rezaloo, B. Rezaei, CoFe2O4/reduced graphene oxide/ionic liquid modified glassy carbon electrode, a selective and sensitive electrochemical sensor for determination of methotrexate, J. Taiwan Inst. Chem. Eng. 78 (2017) 45–50.
[143] Y. Wei, L. Luo, Y. Ding, et al., Highly sensitive determination of methotrexate at poly (L-lysine) modified electrode in the presence of sodium dodecyl benzene sulfonate, Bioelectrochemistry 98 (2014) 70–75.
[144] D. Asbahr, L.C.S. Figueiredo-Filho, F.C. Vicentini, et al., Differential pulse adsorptive stripping voltammetric determination of nanomolar levels of methotrexate utilizing bismuth film modified electrodes, Sensor. Actuator. B Chem. 188 (2013) 334–339.
[145] H. Ghadimi, B. Nasiri-Tabrizi, P.M. Nia, et al., Nanocomposites of nitrogen-doped graphene decorated with a palladium silver bimetallic alloy for use as a biosensor for methotrexate detection, RSC Adv. 5 (2015) 99555–99565.
[146] E. Asadian, S. Shahrokhian, A. Iraji Zad, et al., Glassy carbon electrode modified with 3D graphene–carbon nanotubenetwork for sensitive electrochemical determination of methotrexate, Sensor. Actuator. B Chem. 239 (2017) 617–627.
[147] Y. Guo, Y. Chen, Q. Zhao, et al., Electrochemical sensor for ultrasensitive determination of doxorubicin and methotrexate based on cyclodextrin-graphene hybrid nanosheets, Electroanalysis 23 (2011) 2400–2407.
[148] S. Tesfalidet, P. Geladi, K. Shimizu, et al., Detection of methotrexate in a flow system using electrochemical impedance spectroscopy and multivariate data analysis, Anal. Chim. Acta 914 (2016) 1–6.
[149] F. Wang, Y. Wu, J. Liu, et al., DNA Langmuir–Blodgett modified glassy carbon electrode as voltammetric sensor for determinate ofmethotrexate, Electrochim. Acta 54 (2009) 1408–1413.
[150] F. Wang, Y. Wang, K. Lu, et al., Sensitive determination of methotrexate at nano-Au self-assembled monolayer modified electrode, J. Electroanal. Chem. 674 (2012) 83–89.
[151] L. Janíková-Bandžuchová, R. Šelešovská, Determination of methotrexate at a silver solid amalgam electrode by differential pulse voltammetry, Anal. Lett. 49 (2016) 122–134.
[152] G.A. Saleh, H.F. Askal, I.H. Refaat, et al., A new electrochemical method for simultaneous determination of acyclovir and methotrexate in pharmaceutical and human plasma samples, Anal. Bioanal. Electrochem. 8 (2016) 691–716.
[153] R. Šelešovská, L. Janíková-Bandžuchová, J. Chýlková, Sensitive voltammetric sensor based on boron-doped diamond electrode for determination of the chemotherapeutic drug methotrexate in pharmaceutical and biological samples, Electroanalysis 27 (2015) 42–51.
[154] Z. Chen, S. Qian, X. Chen, et al., Protein-templated gold nanoclusters as fluorescence probes for the detection of methotrexate, Analyst 137 (2012) 4356–4361.
[155] W. Wang, Y.-C. Lu, H. Huang, et al., Facile synthesis of N, S-codoped fluorescent carbon nanodots for fluorescent resonance energy transfer recognition of methotrexate with high sensitivity and selectivity, Biosens. Bioelectron. 64 (2015) 517–522.
[156] Y. Zhao, S. Zou, D. Huo, et al., Simple and sensitive fluorescence sensor for methotrexate detection based on the inner filter effect of N, S co-doped carbon quantum dots, Anal. Chim. Acta 1047 (2019) 179–187.
[157] A.A. Ensafi, P. Nasr-Esfahani, B. Rezaei, Simultaneous detection of folic acid and methotrexate by an optical sensor based on molecularly imprinted polymers on dual-color CdTe quantum dots, Anal. Chim. Acta 996 (2017) 64–73.